Advances in Colloid and Interface Science 162 (2011) 39–58

Contents lists available at ScienceDirect

Advances in Colloid and Interface Science

journal homepage: www.elsevier.com/locate/cis

Kinetics of adsorption of metal ions on inorganic materials: A review

Susmita Sen Gupta [a], Krishna G. Bhattacharyya [b,*]

[a] Department of Chemistry, B N College, Dhubri 783324, Assam, India
[b] Department of Chemistry, Gauhati University, Guwahati 781014, Assam, India

ARTICLE INFO

Available online 12 January 2011

Keywords:
Inorganic adsorbents
Metal ions
Kinetics
Adsorption

ABSTRACT

It is necessary to establish the rate law of adsorbate–adsorbent interactions to understand the mechanism by which the solute accumulates on the surface of a solid and gets adsorbed to the surface. A number of theoretical models and equations are available for the purpose and the best fit of the experimental data to any of these models is interpreted as giving the appropriate kinetics for the adsorption process. There is a spate of publications during the last few years on adsorption of various metals and other contaminants on conventional and non-conventional adsorbents, and many have tried to work out the kinetics. This has resulted from the wide interest generated on using adsorption as a practical method for treating contaminated water. In this review, an attempt has been made to discuss the kinetics of adsorption of metal ions on inorganic solids on the basis of published reports. A variety of materials like clays and clay minerals, zeolites, silica gel, soil, activated alumina, inorganic polymer, inorganic oxides, fly ash, etc. have been considered as the adsorbents and cations and anions of As, Cd, Co, Cr, Cu, Fe, Hg, Mn, Ni, Pb, Se, and Zn as adsorbate have been covered in this review. The majority of the interactions have been divided into either pseudo first order or second order kinetics on the basis of the best fit obtained by various groups of workers, although second order kinetics has been found to be the most predominant one. The discussion under each category is carried out with respect to each type of metal ion separately. Application of models as given by the Elovich equation, intra-particle diffusion and liquid film diffusion has also been shown by many authors and these have also been reviewed. The time taken for attaining equilibrium in each case has been considered as a significant parameter and is discussed almost in all the cases. The values of the kinetic rate coefficients indicate the speed at which the metal ions adsorb on the materials and these are discussed in all available cases. The review aims to give a comprehensive picture on the studies of kinetics of adsorption during the last few years.

Contents

* Corresponding author. Tel.: +91 3612571529; fax: +91 3612570599.
E-mail address: krishna2604@sify.com (K.G. Bhattacharyya).

0001-8686/$ – see front matter © 2011 Elsevier B.V. All rights reserved.
doi:10.1016/j.cis.2010.12.004

1. Introduction

The rates at which metal ions are transferred from the bulk solution to the adsorbent surface and are accumulated there determine the kinetics of adsorption and hence, the efficiency of the adsorption process. The study of kinetics provides an insight into the possible mechanism of adsorption along with the reaction pathways. The residence time of a solute on the adsorbent surface is important in determining whether the process will go to completion or not and also to estimate the total uptake. These are important parameters in designing an actual treatment plant for removing different contaminants from water. It is often very difficult to arrive at an unambiguous rate law, which requires precise knowledge of all the molecular details of the adsorbate–adsorbent interactions, including the energy requirements and stereochemical considerations and also the elementary steps that lead to the adsorption of the solute following a particular mechanism. The process becomes much more complicated when it involves a porous solid with pore diffusion playing an important role. Evaluation of adsorption rate processes yield valuable information about the interactions and have therefore attracted the interests of almost all involved in experimenting with adsorption on solid surfaces from the liquid phase.

It has been universally recognized that adsorption of a species on a solid surface follows three steps, viz., (i) transport of the adsorbate (ions in case of solutions) from the bulk to the external surface of the adsorbent, (ii) passage through the liquid film attached to the solid surface, and (iii) interactions with the surface atoms of the solid leading to chemisorption (strong adsorbate–adsorbent interactions equivalent to covalent bond formation) or weak adsorption (weak adsorbate–adsorbent interactions, very similar to van der Waals forces), in the latter case, desorption may be the ultimate result. In case of porous solids, after passing through the liquid film attached to the external surface, the adsorbate slowly diffuses into the pores and get trapped (adsorbed). It is easily recognized that any of the above steps may be the slowest step determining the overall rate of the interactions and hence the kinetics of the adsorption process. If the step (i) is the slowest, the adsorption will be a transport-limited process (a physical process) and the actual interactions with the solid surface may not be important in determining the adsorption efficiency of the solid. When the step (ii) is the rate determining slowest step, the physical process of diffusion through the liquid film influences the outcome of the process and the efficiency of the solid as an adsorbent can hardly be improved. Only when the step (iii) is the slowest, the adsorption is controlled by a chemical process and the efficiency of the adsorbent can be influenced by suitably controlling the interactions. Usually, the step (i) is the rate-limiting step in systems which are characterized by poor mixing, dilute concentration of adsorbate, small particle size of the adsorbent, etc. In contrast, when dealing with a porous adsorbent, the pore diffusion becomes important when the adsorbate is present in higher concentration, the adsorbent is made of large particles and good mixing is ensured [1–3].

An adsorbent material must have high internal volume accessible to the components being removed from the solvent. Surface area, particularly the internal surface area, pore size distribution and the nature of the pores markedly influence the type of adsorption processes. It is also important that the adsorbent has good mechanical properties such as strength and resistance to destruction and the adsorbent particles are of appropriate size and form. The chemical properties of the adsorbent, namely, degree of ionization at the surface, types of functional groups present, and the degree to which these properties change in contact with the solution are important considerations in determining the adsorption capacity of a solid. The presence of active functional groups on the adsorbent surface allows chemical interactions that usually produce effects different from and less reversible than physical adsorption.

The range of materials chosen as sorbents for treating water contaminated with heavy metals has been truly limitless. While the initial and the continuing trend has been the use of inorganic materials like the clays and the oxides for the purpose, many workers have now turned their attention towards naturally available biomass as the alternative. The emphasis in this review is to consider the rate processes on inorganic materials leading to adsorption of the toxic metal cations and anions and while details have been discussed later, examples of inorganic materials include hydrous ferric oxide [4], simple iron oxide [5], modified Fe_3O_4 [6], modified layered double hydroxide [7], modified SBA-15 [8], and bagasse fly ash [9] from a few recent works.

A careful search of the leading literature resources yields an equally impressive number of bio-materials being experimented as heavy metal scavengers. A few interesting examples have been the

use of peat for Cu(II) [10] and Pb(II) [11], cladophora crispate for Cu (II) [12], aeromonas caviae for Cd(II) [13], green alga spirogyra for Cu (II) [14] and Pb(II) [15], orange waste for Cd(II) [16], cyanobacterium for Cr(VI) [17], alligator weed for Cr(VI) [18], coffee waste for Cr(VI) [19], oedogonium species for Cd(II) [20], Cr(VI) [21] and Ni(II) [22], rice bran for Zn(II) [23], crab shell for As(V) [24], etc.

Several reviews have appeared on water treatment through sorption. Use of chitin and chitosan to remove metal ions from wastewater has been reviewed [25] with particular emphasis on equilibrium studies of sorption capacities and kinetics. Applications of second-order kinetic models to large varieties of adsorption systems were reviewed by Ho [26]. The feasibility of using kaolinite and montmorillonite clay minerals as adsorbents for removal of toxic heavy metals has been reviewed [27]. A good number of works were reported where the modifications of these natural clays were done to carry the adsorption of metals from aqueous solutions. The equilibrium and kinetic studies of heavy metal adsorption on biosorbents, published between 1999 and early 2008, has also been reviewed [28] in which the pseudo-first and -second order equations were considered as the most notable models for describing kinetics. Recently, Gupta et al. [29] have comprehensively reviewed the use of low-cost adsorbents in wastewater treatment. The adsorbents reviewed include alumina, silica gel, zeolite, resin, activated carbon, natural materials like wood, peat, coal, lignite, etc.; industrial/agricultural/domestic wastes or byproducts such as slag, sludge, fly ash, bagasse fly ash, red mud, etc.; and various synthesized products.

The present work gives an overview of the approaches followed by different groups of workers since 2000 in trying to understand the rate processes for adsorption of heavy metals on inorganic adsorbents. The inorganic materials considered were mainly clays and clay minerals, zeolites, silica gel, soil, river sediment, activated alumina, inorganic polymer, red mud, inorganic oxides (viz., hydrous zirconium oxide, titanium oxide, stannic oxide, ferric oxide, etc.), fly ash, etc. Many authors have chemically modified these substances and used the modified materials successfully as adsorbents. To maintain largely 'inorganic' nature of the adsorbents, any material of plant or animal origin is excluded from this review.

2. Kinetics of adsorption: theoretical basis

Kinetics is the study of the rates of chemical processes to understand the factors that influence the rates. Study of chemical kinetics includes careful monitoring of the experimental conditions which influence the speed of a chemical reaction and hence, help attain equilibrium in a reasonable length of time. Such studies yield information about the possible mechanism of adsorption and the different transition states on the way to the formation of the final adsorbate–adsorbent complex and help develop appropriate mathematical models to describe the interactions. Once the reaction rates and the dependent factors are unambiguously known, the same can be utilized to develop adsorbent materials for industrial application and will be useful in understanding the complex dynamics of the adsorption process.

The rates depend on the concentrations of the species involved in the adsorption process and the conventional rate law may be of the form,

$$R = k[A]^a[B]^b \ldots\ldots \quad (1)$$

where k is the rate coefficient, a, b … etc., represent the order with respect to the species, A, B, etc. The exact form of the rate law can give some information about the mechanism of the reaction.

2.1. Lagergren pseudo first order model

The Lagergren equation is probably the earliest known example describing the rate of adsorption in the liquid-phase systems. This equation [30] has been one of the most used equations particularly for pseudo first order kinetics:

$$dq_t / dt = k_1(q_e - q_t) \quad (2)$$

where k_1 (min^{-1}) is the pseudo first order adsorption rate coefficient. The integrated form of the Eq. (2) for the boundary conditions of $t = 0$, $q_t = 0$ and $t = t$, $q_t = q_t$,

$$ln(q_e - q_t) = ln\, q_e - k_1 t \quad (3)$$

where q_e and q_t are the values of amount adsorbed per unit mass at equilibrium and at any time t. The values of k_1 can be obtained from the slope of the linear plot of $\ln(q_e - q_t)$ vs. t

It is necessary to know the value of q_e for fitting the experimental data to the Eq. (3). Determining q_e accurately is a difficult task, because in many adsorbate–adsorbent interactions, the chemisorption becomes very slow after initial fast response and it is difficult to ascertain whether equilibrium is reached or not. In such cases, an approximation has to be made about q_e introducing an element of uncertainty in the calculations. It is possible that the amount adsorbed even after a long interaction time (taken as equivalent to equilibrium) is still appreciably smaller than the actual equilibrium amount [31]. For many adsorption processes, the Lagergren pseudo first order model is found suitable only for the initial 20 to 30 min of interaction and not fit for the whole range of contact time [32]. The value of k_1 depends on the initial concentration of the adsorbate that varies from one system to another. It usually decreases with the increasing initial adsorbate concentration in the bulk phase [33,34]. When considering the influence of pH and temperature on the k_1 value, the estimation of the adsorption rate cannot be done when only the equilibrium data are at disposal [35].

The real test of the validity of Eq. (3) arises from a comparison of the experimentally determined q_e values and those obtained from the plots of $\ln(q_e - q_t)$ vs. t [32,36]. If this test is not valid, then higher order kinetic models are to be tested with respect to the experimental results. If the Lagergren equation does not fit well in the whole range of interaction time [32], obviously the adsorption process is following a much more complex mechanism than the one on the basis of simple first order kinetics.

2.2. Pseudo-second order model

The second order kinetics may be tested on the basis of the equation [37],

$$dq_t / dt = k_2(q_e - q_t)^2 \quad (4)$$

where k_2 is the second order rate coefficient. Separation of the variables followed by integration and application of the boundary conditions ($q_t = 0$ at $t = 0$ and $q_t = q_t$ at $t = t$) yields a linear expression of the form

$$t / q_t = 1 / \left(k_2 q_e^2\right) + (1 / q_e) \cdot t \quad (5)$$

k_2 often depends on the applied operating conditions, namely, initial metal concentration, pH of solution, temperature and agitation rate, etc. [35,38]. The integral form of the model, represented by the Eq. (5) predicts that the ratio of the time/adsorbed amount should be a linear function of time [39].

Both theoretical investigations [40,41] and the experimental studies [38,42] indicate that the value of k_2 usually depends on the initial adsorbate concentration in the bulk phase. The rate coefficient, k_2 decreases with the increasing initial adsorbate concentration as a rule, where k_2 is interpreted as a time-scaling factor. Thus, higher is the initial concentration of adsorbate, the longer time is required to

reach an equilibrium, in turn, the k_2 value decreases [34,43,44]. Due to the complexity of the problem and numerous different factors, the influence of pH and temperature on k_2 has not yet been theoretically studied. The influence of both pH and temperature is not restricted to the equilibrium features of the system but these factors play an important role in the course of kinetic processes [45–47]. While considering all the factors which may control the rate of the adsorption process, the significance of the transport of adsorbate in the subsurface region can be identified by using different degrees of mechanical mixing during the experiment. At higher agitation rates, the volume of the subsurface layer reaches a constant minimum while the rate of solute transport within it reaches a constant maximum value and can be usually neglected.

The initial adsorption rate, h, of a second order process as $t \to 0$ is defined as,

$$h = k_2 q_e^2. \tag{6}$$

The initial adsorption rate, h, adsorption capacity, q_e, and the pseudo-second order rate coefficient, k_2, can be determined experimentally from the slope and intercept of a plot of t/q_t against t. In applying Eqs. (5) and (6) to the experimental data, it is essential to have a precise knowledge of the equilibrium adsorption capacity, q_e [11].

The pseudo-second order equation has also been interpreted as a special kind of Langmuir kinetics [48]. This line of interpretation assumes that (i) the adsorbate concentration is constant in time and (ii) the total number of binding sites depends on the amount of adsorbate adsorbed at equilibrium. One of the advantages of the pseudo-second order equation for estimating the q_e values is its small sensitivity for the influence of the random experimental errors.

2.3. Elovich equation

The Elovich equation assumes that the actual solid surfaces are energetically heterogeneous and that neither desorption nor interactions between the adsorbed species could substantially affect the kinetics of adsorption at low surface coverage. The crucial effect of the surface energetic heterogeneity on adsorption equilibria in the gas/solid systems has been demonstrated by [49], but the extension of the same to liquid/solid system is not known. The Elovich Equation [50,51] has been used in the form,

$$dq_t / dt = \alpha \, exp(-\beta \, q_t) \tag{7}$$

with the Elovich coefficients, α and β. Assuming $\alpha\beta t \gg 1$, and $q_t = 0$ at $t = 0$ and $q_t = q_t$ at $t = t$, the linear form of the Eq. (7) is given by [52],

$$q_t = \beta \, ln(\alpha\beta) + \beta \, ln \, t. \tag{8}$$

It is postulated that the Elovich coefficients, α and β, represent the initial adsorption rate (g mg^{-1} min^{-2}) and the desorption coefficient (mg g^{-1} min^{-1}) respectively. The Elovich coefficients could be computed from the plots of q_t vs. ln t.

For longer adsorption time [i.e. $t \to \infty$] the non-physical behaviour of Eq. (8) can be observed which is due to neglecting the rate of simultaneously occurring desorption. Thus, in practice, the applicability of the Elovich equation is restricted to the initial part of the adsorbate–adsorbent interaction process, when the system is relatively far from equilibrium. Rudzinski and Plazinski [39] has quantitatively proved that both the pseudo-second order and the Elovich equations exhibit essentially identical behaviour when considering the values of the fractional surface coverage lower than about 0.7.

2.4. Intra-particle diffusion

For porous adsorbents, the diffusion of the adsorbate molecules or ions into the pores is also to be taken into account in finding a suitable kinetic model for the process. In many cases, the intra particle diffusion may control the rate of uptake of an adsorbate, which is represented by the following familiar expression [53–55],

$$q_t / q_e = 1 - (6/\pi^2)\Sigma\left(1/n^2\right) \, exp\left(-n^2\pi^2 D_c t / r^2\right) \tag{9}$$

the ratio, q_t/q_e, giving the fractional approach to equilibrium, D_c = intra-crystalline diffusivity, r = particle radius, t = reaction time, and the summation is carried out from $n = 1$ to $n = \alpha$.

The Eq. (9) can be rewritten in the following simplified form,

$$1 - q_t / q_e = (6/\pi^2) \, exp(-\pi^2 D_c / r^2) t \tag{10}$$

or,

$$ln(1 - q_t / q_e) = (-\pi^2 D_c / r^2) t + \; ln(6/\pi^2). \tag{11}$$

Therefore, the plot of $\ln(1 - q_t/q_e)$ versus t should be linear with a slope of $(-\pi^2 D_c/r^2)$, which is known as the diffusion time constant. The slope can be expressed as:

$$k' = \pi^2 D_c / r^2 \tag{12}$$

where, k′ is the overall rate constant, inversely proportional to the square of the particle radius.

Weber and Morris [56] introduced a simpler expression to obtain the diffusion rate coefficient, k_i,

$$q_t = k_i \cdot t^{0.5}. \tag{13}$$

The significant feature of this expression is that the linear plots of q_t vs. $t^{0.5}$ should pass through the origin (zero intercept). Thus the intra-particle diffusion model can be easily tested through the above plots provided they have zero intercept, which indicates a controlling influence for the diffusion process on the kinetics. The rate coefficient, k_i (mg g^{-1} $min^{-0.5}$) could be obtained from the slope of the plots.

It is to be noted that the Eq. (13) represents a simplistic approximation of the pore diffusion kinetics without considering the possible impacts of the pore dimensions. The literature is mostly silent on these aspects and few works have appeared reporting a detailed study of the impact of pore diffusion processes on heavy metal uptake, and in particular, the effects of pore radius and pore size on the sorption kinetics.

2.5. Liquid film diffusion

When the flow of the reactant through the liquid film surrounding the adsorbent particles is the slowest process determining kinetics of the rate processes, the liquid film diffusion model [57] given by the simple relation,

$$ln(-F) = -k_{fd} t \tag{14}$$

could be the appropriate way to characterize the kinetics. F is the fractional attainment of equilibrium ($= q_t/q_e$) and k_{fd} (min^{-1}) is the film diffusion rate coefficient. A linear plot of $-\ln(1-F)$ vs. t with zero intercept suggests that the kinetics of the adsorption process is controlled by diffusion through the liquid film.

Film diffusion kinetics and its influence on adsorption rate processes, with relation to attaining equilibrium, is also an area receiving very little attention of the adsorption scientist. It is possible that the transport process delivering the solute to the sorbent surface is considered less important than the process of actually binding the

solute to the sorbent. Although this binding may be quite weak as found in many cases where some thermodynamic data are available, and might be physical in nature or might have involved ion-exchange type interactions, a large number of studies invariably consider the binding to be chemical in nature.

2.6. Azizian modification of pseudo-first order and pseudo-second order models

Azizian [40] derived pseudo-first order and pseudo-second order models by a general and different method. The author also characterized the reaction conditions under which the models must be used and to derive the related rate coefficients. Considering the adsorption and desorption of solute A in solution,

$$A + \square \underset{k_d}{\overset{k_a}{\leftrightarrow}} A_{(a)} \tag{15}$$

where k_a and k_d are the adsorption and desorption rate coefficients, and □ represents the vacant site. If θ is the surface coverage fraction ($0<\theta<1$) and C is the molar concentration of adsorbate at any time, the adsorption and desorption rates can be written as [58],

$$\upsilon_a = k_a C(1-\theta) \tag{16}$$

$$\upsilon_d = k_d \theta. \tag{17}$$

The overall rate equation is,

$$d\theta / dt = \upsilon_a - \upsilon_d \tag{18}$$

$$d\theta / dt = k_a C(1-\theta) - k_d \theta. \tag{19}$$

By adsorption, the concentration of solute in solution decreases. Thus,

$$C = C_0 - \beta\,\theta \tag{20}$$

where C_0 is the initial molar concentration of adsorbate, C is its molar concentration at any time. The β is given by,

$$\beta = (C_0 - C_e) / \theta_e \tag{21}$$

where C_e is the equilibrium molar concentration of solute and θ_e is the equilibrium coverage fraction. By inserting Eq. (20) into Eq. (19),

$$d\theta / dt = k_a(C_0 - \beta\theta)\ (1-\theta) - k_d \theta. \tag{22}$$

Azizian [40] used the Eq. (22) for derivation of various kinetic models of adsorption at different conditions. The advantage of the Azizian derivation is that when the initial concentration of adsorbate is too high compared to βθ, then the adsorption process obeys pseudo-first order kinetics, and when the initial concentration of adsorbate is comparable to βθ, then it follows a pseudo-second order path. The rate constant of the pseudo-second order model is a complex function of the initial concentration of the solute.

2.7. Validity of a model

It has been the practice of the workers to test various kinetic models in order to derive some insight into the actual adsorption process. The validity of a model may be quantitatively checked by using a normalized standard deviation Δq (%) calculated by the following equation [59,60],

$$\Delta q\,(\%) = \sqrt{\frac{\sum\left[\left(q_{exp} - q_{cal}\right)/q_{exp}\right]^2}{n-1}} \times 100$$

where, q_{exp} and q_{cal} are the experimental and calculated amount of metal ion adsorbed per unit mass of adsorbent at equilibrium and n is the number of data points.

3. Experimental insight into kinetics of adsorption

Adsorption mechanisms depend on the characteristics of the adsorbate and adsorbent, adsorbate–adsorbent interactions and the system conditions like pH, temperature, etc. The interactions may also involve the solvent molecules and the attractive forces may be of different nature. Such forces usually act in concert, but one particular type may be more dominant in a particular situation. The differential distribution of the solute molecules or ions between the liquid and the solid phases results from their relative affinity for each phase, which in turn relates to the nature of the forces that exist between the molecules of the adsorbate and those of the solvent and adsorbent phases. The intermolecular forces of the molecules at the surface of the adsorbent rather than the bulk phase molecules, are involved in the adsorption process and the interactions manifest over a broad range [61]. The first order kinetic processes signify reversible interactions with an equilibrium being established between liquid and solid phases [62] whereas the second order kinetic model assumes that the rate-limiting step [62,63] is most likely to involve chemical interactions leading to binding of the ions to the surface by bonding as strong as covalent bonding. These two models have been widely tested by various workers and conformity to either of the models or both have been reported in the literature. Other models of kinetics have also been applied with limited or qualified success.

Importance in kinetic studies has been one of the major features of recent studies in adsorption. However, many of the studies were without application of any kinetic models and were based on just showing the variation in adsorption capacity with time and usually to establish the time taken to arrive at equilibrium. A cross-section of such works that considered adsorption on various inorganic solids without dealing with any of the kinetic aspects is given below:

Cu(II) on Ca-kaolinite [64], Cd(II), Cu(II) and Pb(II) on diatomite and Mn-diatomite [65], Ca(II) on hydroxy-Al pillared montmorillonite [66], Cd(II), Cr(III), Cu(II), Ni(II), Pb(II) and Zn(II) on kaolinite and illite [67], Cu(II) on sewage sludge ash [68], Ni on illite [69], Cd(II), Cr(III), Cu(II), Mn(II), Ni(II), Pb(II) and Zn(II) on Na-montmorillonite [70], As(V) on calcined synthetic hydrotalcite and calcined natural boehmite [71], Cd(II) and Zn(II) on apatite [72], Co(II), Cu(II), Mn(II) and Zn(II) on natural zeolite [73], Cu(II), Pb(II) and Zn(II) on natural zeolite [74], As(V) on bimetal oxide [75], Cd(II) and Pb(II) on amine-modified zeolite [76], As(III) and As(V) on TiO_2 [77], Cd(II) and Zn(II) on modified clinoptilolite [78], Co(II) and Zn(II) on treated bentonite [79], Cu(II) on clinoptilolite [80], Cu(II), Co(II) and Zn(II) on natural bentonite [81], Cr(III) on zeolite [82], Cr(VI) on surfactant-modified zeolite [83], Co(II) and Ni(II) on ion exchange resins [84], Hg(II) on natural and modified montmorillonite (treated with pyridine, dimethyl sulfoxide and 3-aminopropyltriethoxysilane) [85], Cd(II), Cr(III) and Mn(II) on natural sepiolite [86], Cu(II) on Serbian zeolite, clay and diatomite [87], Cu(II) on bentonite–polyacrylamide composites [88], etc.

Other works that found the equilibrium adsorption time, but have not gone into the kinetics during the last few years include the following (the equilibrium time is given in the parenthesis):

Cd(II), Cu(II) and Pb(II) on smectites (30 min) [89], Cu(II) and Pb (II) on electric furnace slag (480 min) [90], Cd(II) and Cr(VI) on fly ash (120 min) [91], Cu(II), Ni(II) and Zn(II) on Turkish fly ash (120 min) [92], Cr(III) on bentonite and perlite (30 min for bentonite and 900 min for perlite) [93], Co(II) on sepiolite

(120 min) [94], Cr(III), Fe(III), Zn(II) and Mn(II) on modified silica gel (20–30 min) [95], Cr(VI) on hydrous titanium oxide (30 min) [96], Hg(II), Pb(II) (90 min) and Cd(II) (75 min) on cation exchanger [97], Cd(II) and Zn(II) on low-grade phosphate (30 min) [98], Cu(II) and Zn(II) on SBA-15 (60 min) [99], Pb(II) on calcium hydroxyapatite (20 min) [100], Cr(III) and Pb(II) on a local clay (30 min) [101], Cu(II) on zero-valent iron (180 min) [102], Cd(II), Pb(II) and Zn(II) on a local clay (180 min) [103], Pb (II) on alginate salts (60 min) [104], Ag(II), Co(II), Cu(II), Ni(II) and Pb(II) (30 min) [105], Cr(III), Fe(III), Mn(II) and Zn(II) on ion-imprinted amino-functionalized silica gel (<60 min) [106], Cd(II) on Tunisian palygorskite (40 min) [107], etc.

Many other authors have attempted to apply one or more kinetic models to their experimental data and commented on the suitability or otherwise of the same. The following discussion is based on the specific kinetic model that was found to conform to the experimental results.

3.1. First order kinetics

Literature reports on adsorption of metal ions on a large number of inorganic materials have shown compliance with the first order model of kinetics. A collection of these works is given in Table 1 (Appendix) that also includes values of the first order rate coefficient, experimental conditions, and time to attain equilibrium. A brief discussion of the results is given below with respect to each metal ion.

3.1.1. Arsenic

Adsorption of anionic As(V) on aluminium loaded zeolite was also shown to follow first order kinetics by [108] with an increase in the rate of adsorption from 3.8×10^{-2} to 10.6×10^{-2} min^{-1} as the adsorbent dose was increased from 1.25 to 5 g L^{-1} (experimental conditions: adsorbent 1.25 g L^{-1}, 2.5 g L^{-1}, and 5.0 g L^{-1}, As(V) 0.13 mM, and temperature 297 K).

Adsorption of As(III) and As(V) anions on activated, neutralized red mud attained equilibrium at 360 min and 180 min, respectively [109]. The linear curves obtained for both the species indicated the first-order nature of the adsorption process and suggested that the process depends on both the solution concentration and the number of available adsorption sites. The Lagergren first order rate coefficients were comparatively larger for As(III) than As(V) (experimental conditions: adsorbent 5.0 g L^{-1}, As(V) 20.37 μm and As(III) 14.82 μm, pH 7.0, and temperature 296 K). The rate of adsorption of As(III) on zero-valent iron (As(III) 1.0 mg L^{-1}, adsorbent 0.5, 2.5, 5.0, 7.5, and 10.0 g L^{-1}, pH 7.0, and temperature 298 K) showed more than 80% removal within 7 min and ~99.9% within 60 min [110]. The first-order rate coefficients varied from 0.07 min^{-1} to 1.30 min^{-1} for the adsorbent concentration of 0.5 to 10.0 g L^{-1}. In another work [111], a mixture of china clay and fly ash was used for adsorption of As (III) from water. The process reached equilibrium within 120 min. The first order rate coefficients increased from 2.19×10^{-2} min^{-1} to 2.26×10^{-2} min^{-1} as the temperature changes from 303 to 323 K (experimental condition: As(III) 5.0 mg L^{-1}, particle size <53 μm, pH 8.0, and temperature 303 to 323 K).

3.1.2. Aluminium

Adsorption of Al(III) has not received wide attention. In one significant work, Al(III) was adsorbed onto powdered marble waste [112] at various initial metal ion concentrations. The adsorption was quite rapid in the first stage, but with the passage of time, the rate of adsorption decreased and ultimately reached equilibrium. The equilibrium time was of 5 min for initial concentrations of 1.0 and 3.0 mg L^{-1}, 25 min for those of 4.0 and 8.0 mg L^{-1} and 70 min for those having more than 10.0 mg L^{-1} of metal ions. The adsorption process was shown to follow the Lagergren first order model with a rate coefficient of 0.0795 min^{-1} (adsorbent 100 mg L^{-1}, pH 7.0, and temperature 298 K).

3.1.3. Cadmium

Adsorption of Cd(II) on red mud (an aluminium industry waste) was reported to follow the first order kinetics with rate constant of 3.47×10^{-3} min^{-1} (experimental conditions: adsorbent 10.0 g L^{-1}, Cd(II) 8.89×10^{-4} M, and pH 4.0) [113].

The removal of Cd(II) on silico-antimonate (an inorganic ion exchange material) was shown to obey Lagergren model [114] of kinetics. The first order rate coefficient had a value of 2.42×10^{-2} min^{-1} (experimental conditions: adsorbent 5.0 g L^{-1}, Cd(II) 50 mg L^{-1}, pH 4.0, and temperature 298 ± 1 K). The same group of workers carried out batch kinetic studies for adsorption of Cd(II) ions from aqueous waste solutions on iron(III) titanate [115] and showed that the equilibrium was attained within 180 min conforming to a linear relationship between ln $(q_e - q_t)$ and t, and therefore, confirming first order kinetics for Cd(II)–iron(III) titanate interactions (experimental conditions: adsorbent 10.0 g L^{-1}, Cd(II) 50 mg L^{-1}, pH 4.3, and temperature 298 ± 1 K) although the rate coefficient value was not reported.

Adsorption of Cd(II) from aqueous solution on sodium dodecyl-sulfate-montmorillonite (SDS-Mt) and hydroxyl-alumino-silicate-montmorillonite (HAS-Mt) [116] was also shown to be first order in kinetics with the rate coefficient for HAS-Mt higher than that of SDS-Mt (adsorbent 10.0 g L^{-1}, Cd(II) 20 to 200 mg L^{-1}, pH 5.0, stirring speed 3000 rpm, and temperature 298 K).

Cd(II) adsorption by non-activated and activated $AlPO_4$ [117] attained equilibrium within 120 min for the former and 180 min for the latter. The activation of $AlPO_4$ created pores and consequently, the mechanism of Cd(II) uptake changed. The kinetics continued to follow Lagergren first order model and the rate coefficients in the temperature range of 303 to 323 K varied from 21.42×10^{-3} to 26.94×10^{-3} min^{-1} for Cd(II)–$AlPO_4$ and from 12.90×10^{-3} to 23.95×10^{-3} min^{-1} for Cd (II)-activated $AlPO_4$ (adsorbent 6.67 g L^{-1}, pH 6.0, and temperature 303 to 323 K).

3.1.4. Chromium

The adsorption of Cr(VI) on red mud had followed first order kinetics [118]. Nearly 30 to 45% of the adsorption capacity was realized within the first hour of contact, however, the equilibrium was reached in 8 to 10 h (experimental conditions: adsorbent 10.0 g L^{-1}, particle size 150–200 mesh, Cr(VI) 5.77×10^{-3} M, and temperature 303 K). Similarly, Cr(VI) was taken up by IRN77 cation-exchange resin in a first order mechanism [119], although the rate coefficient (97.70×10^{-2} to 97.81×10^{-2} min^{-1}) was not influenced much by the initial metal ion concentrations (experimental conditions: adsorbent 2.0 g L^{-1}, pH 5.3, Cr(VI) 50 to 150 mg L^{-1}, and temperature 298 K).

Banerjee et al. [120] studied kinetics of adsorption of Cr(VI) on fly ash, FA (solid waste from thermal power plant) and impregnated fly ash, IFA-Al and IFA-Fe [impregnated with 0.1 M $Al(NO_3)_3$ and 0.1 M $Fe(Cl)_3$ respectively]. The rate coefficient varied from 0.111 to 0.167 min^{-1} for FA, 0.176 to 0.230 min^{-1} for IFA-Al and 0.167 to 0.216 min^{-1} for IFA-Fe in the temperature range of 303 to 333 K (experimental conditions: adsorbent 3.33 g L^{-1}, stirring speed 100 rpm, and temperature 303 to 333 K).

Adsorption of Cr(III) from aqueous solution on sodium dodecyl-sulfate-montmorillonite (SDS-Mt) and hydroxyl-alumino-silicate-montmorillonite (HAS-Mt) [116] was also shown to be following first order kinetics with the first order rate coefficient having higher values in case of HAS-Mt than in SDS-Mt. (experimental conditions: adsorbent 10.0 g L^{-1}, Cr(III) 20 to 200 mg L^{-1}, pH 5.0, stirring speed 3000 rpm, and temperature 298 K).

Three kinds of organo-modified rectorite, viz, dodecyl benzyl dimethyl ammonium rectorite (OREC1), hexadecyl trimethyl

ammonium rectorite (OREC2), and octadecyl trimethyl ammonium rectorite (OREC3) were used by Huang et al. [121] for adsorption of Cr (VI) from aqueous solution. Rapid adsorption took place in the first 30 min and equilibrium was attained within 40 min. OREC3 had the highest value for the first order rate coefficient (1.95×10^{-2} min^{-1}) (experimental conditions: adsorbent 1.0 g L^{-1}, Cr(VI) 100 mg L^{-1}, pH 6.0, and temperature 299 K). Removal of Cr(VI) by spent activated clay [122] was also very rapid with approximately 95% of the adsorption over within 60 min. The adsorption process required 120 min to reach equilibrium and followed Lagergren first order kinetics. The rate coefficient increased with decreasing pH and increasing temperature. Thus, for increase in pH from 2.0 to 4.0, the rate coefficient varied from 0.056 to 0.030 min^{-1}, 0.064 to 0.041 min^{-1}, 0.075 to 0.051 min^{-1} and 0.178 to 0.070 min^{-1} at 277, 287, 297 and 313 K. The high correlation coefficient (>0.99) and the low standard deviation values (<10.5%) indicated that the experimental data were well correlated to the first order model. It appears that the rate of Cr(VI) adsorption speeded up under acidic conditions. At low pH value, specifically less than pH_{zpc} (3.8 in this study), the adsorbent surface was negatively charged, enhancing the adsorption of anionic Cr(VI) by means of electrostatic attraction. As the pH increased, the attractive forces become smaller and this consequently results in decrease of adsorption (experimental conditions: adsorbent 1.0 g L^{-1}, Cr(VI) 6.75 mg L^{-1}, stirring speed 300 rpm, pH 2.0 to 4.0, and temperature 277 to 313 K).

The use of takovite–aluminosilicate nanocomposite for adsorption of Cr(III) also resulted in first order kinetics (experimental conditions: adsorbent 20.0 g L^{-1}, Cr(III) 6 μ mol ml^{-1}, pH 3.2, and temperature 298 K) [123].

3.1.5. Cobalt

Co(II) adsorption has been explored only to a limited extent. Uptake of Co(II) on IRN77 cation-exchange resin was reported to follow first order kinetics [119]. The rate constant was influenced by the initial metal ion concentration and varied from 98.62×10^{-2} to 98.71×10^{-2} min^{-1} (experimental conditions: adsorbent 2.0 g L^{-1}, pH 5.3, Co (II) 50 to 150 mg L^{-1}, and temperature 298 K). Adsorption of Co(II) on Turkish kaolinite required 120 min to reach equilibrium [124]. The first order rate coefficient increased from 2.40×10^{-3} to 3.80×10^{-3} min^{-1} for an increase in temperature from 298 to 313 K (experimental conditions: adsorbent 1.0 g L^{-1} and particle size 200 mesh).

3.1.6. Copper

Lin and Juang [125] modified montmorillonite with sodium dodecylsulfate and used the modified clay for adsorption of Cu(II). The adsorption was rapid during the first 10 min and equilibrium was attained within 120 min. The first order plots gave the standard deviation of 1.2%. The high capacity and fast kinetics indicated that the modified clays had better potential for treatment of industrial effluents contaminated with trace amounts of heavy metals (experimental conditions: adsorbent 2.0 g L^{-1}, Cu(II) 0.78 mM, and temperature 298 K). Adsorption of Cu(II) on Turkish kaolinite required 120 min to reach equilibrium [124]. The first order rate coefficient increased from 5.10×10^{-3} to 9.00×10^{-3} min^{-1} in the temperature range of 298 to 313 K (experimental conditions: adsorbent 1.0 g L^{-1} and particle size 200 mesh). The adsorption of Cu(II) on silico-antimonate was also in conformity with the first order kinetic model [114] with a rate coefficient of 2.19×10^{-2} min^{-1} (experimental conditions: adsorbent 5.0 g L^{-1}, Cu(II) 50 mg L^{-1}, pH 4.0, and temperature 298 ± 1 K).

Adsorption of Cu(II) from aqueous solution on sodium dodecyl-sulfate-montmorillonite (SDS-Mt) and hydroxyl-alumino-silicate-montmorillonite (HAS-Mt) [116] has been proposed to follow first order kinetics. The first order rate coefficient has a higher value in case of HAS-Mt than in SDS-Mt (experimental conditions: adsorbent 10.0 g L^{-1}, Cu(II) 20 to 200 mg L^{-1}, pH 5.0, stirring speed 3000 rpm, and temperature 298 K).

The use of powdered limestone for Cu(II) adsorption needed 40 min to reach equilibrium with the first order rate coefficient of 3.1×10^{-2} min^{-1} (r ~ 0.99) (experimental conditions: adsorbent 8.0 g L^{-1}, pH 7.0, stirring speed 250 rpm, and temperature 298 K) [126]. Karamanis and Assimakopoulos [127] prepared a series of aluminium-pillared montmorillonite by varying OH/Al ratio and used these pillared materials for the adsorption of Cu(II). The adsorption process was very fast and attained equilibrium within 20 min. The rate coefficient of Cu(II) adsorption on the pillared sample was higher than that on the parent montmorillonite. This result is attributed to the easiness of pore accessibility due to the three-dimensional structure of pillared clays than the blocking of the pores after the initial adsorption of Cu(II) within the montmorillonite interlayer space and the subsequent collapse of the aluminosilicate clay sheets. It is clear from the kinetic measurements that the velocity of transport of Cu(II) from the liquid phase to solid phase is rapid enough for application of pillared clays in the treatment of polluted water.

Tofan et al. [128] have found that adsorption of Cu(II) ions from water on fly ash is influenced by initial Cu(II) concentration. When the initial concentration of Cu(II) is increased from 30 mg L^{-1} to 100 mg L^{-1}, the rate coefficient has increased from 3.45×10^{-3} min^{-1} to 5.07×10^{-3} min^{-1} (r ~ 0.99) in line with first order kinetics (experimental conditions: adsorbent 10.0 g L^{-1}, Cu(II) 30–100 mg L^{-1}, pH 4.5, and temperature 291 K).

3.1.7. Lead

First order kinetics was reported for adsorption of Pb(II) on low grade carbonate rock phosphate (CRP) and hydroxy aluminosilicate based mineral pyrophyllite (SP) in aqueous solution [129]. The first order rate coefficient varied from 247.00×10^{-3} min^{-1} to 56.50×10^{-3} min^{-1} for CRP and from 151.90×10^{-3} min^{-1} to 34.60×10^{-3} min^{-1} for SP for Pb(II) concentration range of 5 to 500 mg L^{-1}. The rate coefficients decreased with increase in the initial concentration; but CRP had a higher rate coefficient than SP (experimental conditions: CRP 5.0 g L^{-1} and SP 10.0 g L^{-1}, Pb(II) 5 to 500 mg L^{-1}, and temperature 298 K). The adsorption of Pb(II) on red mud [118] followed first order kinetics with 30 to 45% of the adsorption capacity realized within the first hour of contact, but the equilibrium was reached only after 8 to 10 h. (experimental conditions: adsorbent 10.0 g L^{-1}, particle size 150–200 mesh, Pb(II) 3.38×10^{-3} M, and temperature 303 K).

When beach sand was used for adsorption of Pb(II) [130], the interactions were again found to follow first order kinetics with a rate coefficient of 0.13 ± 0.01 min^{-1} (r ~ 0.9861) (experimental conditions: adsorbent 1.33 g L^{-1}, Pb(II) 9.65×10^{-6} M, and temperature 303 K). The uptake of Pb(II) on Haro river sand was also shown to be very fast as the process required only 10 min to get to equilibrium [131]. The first order rate coefficient was of 0.2046 min^{-1} (experimental conditions: adsorbent 10.0 g L^{-1}, Pb(II) 4.82×10^{-5} M, stirring speed 700 rpm, and temperature 298 ± 2 K).

Pb(II) adsorption on vermiculite was very fast and more than 90% Pb (II) uptake was within the first 10 min with the equilibrium being attained within 30 min. The forward and backward rate coefficients were reported as 0.1113 min^{-1} and 0.003918 min^{-1}, respectively (experimental conditions: Pb(II) 20 mg L^{-1}, adsorbent 4.0 g L^{-1}, pH 5.0, and stirring 1200 rpm) [132]. In another work, adsorption of Pb(II) on carbonate-hydroxyapatite was a complicated non-homogeneous solid/water interaction [133] where after being very fast initially, the interactions slowed down as a whole agreeing with first-order kinetic equation. Solution pH, temperature, adsorbent dose and initial concentration of Pb(II) influenced the values of the rate coefficient. There was positive linear relationship between the rate coefficient and adsorbent dose, solution pH and temperature.

The removal of Pb(II) by adsorption on takovite–aluminosilicate nanocomposites was found to attain equilibrium very sharply within 20 min with first order rate coefficient of 0.086 min^{-1} (experimental

conditions: adsorbent 20.0 g L^{-1}, Pb(II) 8 μmol ml^{-1}, pH 4.5, and temperature 298 K) [123].

3.1.8. Manganese

Adsorption of Mn(II) on Turkish kaolinite required 120 min to reach equilibrium [124]. In the solution temperature range of 298 to 313 K, the first order rate coefficient increased from 1.20×10^{-3} to 1.90×10^{-3} min^{-1} (experimental conditions: adsorbent 1.0 g and particle size 200 mesh).

3.1.9. Mercury

Banerjee et al. [120] have found that adsorption of Hg(II) on fly ash (FA) and impregnated fly ash [impregnated with 0.1 M $Al(NO_3)_3$; IFA-Al and 0.1 M $Fe(Cl)_3$; IFA-Fe] followed first order kinetics with the rate coefficient varying from 0.118 to 0.158 min^{-1} for FA, 0.141 to 0.191 min^{-1} for IFA-Al and 0.165 to 0.204 min^{-1} for IFA-Fe in the temperature range of 303 to 333 K. The values indicate that Hg(II) interacts quite fast with the fly ash and modified fly ash surfaces and this rate increases further at higher temperature (experimental conditions: adsorbent 3.33 g L^{-1}, stirring speed 100 rpm, and temperature 303 to 333 K).

3.1.10. Nickel

Ni(II) uptake on IRN77 cation-exchange resin takes place through a first order kinetic mechanism [119] and accordingly, the rate coefficient was influenced by the initial metal ion concentration (experimental conditions: adsorbent 2.0 g L^{-1}, Ni(II) 50 to 150 mg L^{-1}, pH 5.3, and temperature 298 K).

Similarly, with fly ash (FA) and impregnated fly ash [with 0.1 M Al $(NO_3)_3$; IFA-Al and 0.1 M $Fe(Cl)_3$; IFA-Fe], Ni(II), adsorption of Ni(II) from aqueous solution [134] had first order rate coefficient of 0.299 to 0.097 min^{-1} for FA, 0.391 to 0.111 min^{-1} for IFA-Al and 0.332 to 0.101 $kmin^{-1}$ for IFA-Fe in the temperature range of 303 to 333 K. It thus appears that Ni(II) uptake was very fast at a lower temperature compared to those in a higher temperature (experimental conditions: adsorbent 1.25 g L^{-1}, Ni(II) 20 mg L^{-1}, pH 6.0, and stirring speed 100 rpm). Adsorption of Ni(II) on silico-antimonate has also been proposed as following the Lagergren model [114] with a first order rate coefficient of 4.15×10^{-2} min^{-1} (experimental conditions: adsorbent 5.0 g L^{-1}, Ni(II) 50 mg L^{-1}, pH 4.0, and temperature 298 ± 1 K). When using Turkish kaolinite as an adsorbent for Ni(II), Yavuz et al. [124] have noticed that the interactions are best described by a first order mechanism and the rate coefficient had values from 3.00×10^{-3} to 8.50×10^{-3} min^{-1} in the temperature interval of 298 to 313 K (experimental conditions: adsorbent 1.0 g L^{-1} and particle size 200 mesh).

The first order kinetic model also fitted very well with the experimental data for the adsorption of Ni(II) on TiO_2 [135]. About 94.0% of Ni(II) was taken up within 20 min by the adsorbent. When the adsorption was carried out in a temperature range of 288 to 318 K, there is a corresponding increase in the rate coefficient from 14.6 to 38.1 min^{-1} (Ni(II) 10 mg L^{-1}), 11.5 to 40.2 min^{-1} (Ni(II) 30 mg L^{-1}) and 11.3 to 36.3 min^{-1} (Ni(II) 50 mg L^{-1}) (experimental conditions: adsorbent 1.0 g L^{-1}, Ni(II) 10, 30, and 50 mg L^{-1}, pH 5.0 ± 0.1, and stirring speed 300 ± 5 rpm).

Heidari et al. [136] prepared amino functionalized MCM-41 (NH_2-MCM-41) for adsorption of Ni(II) from aqueous solution and showed that the adsorption rate decreased with an increase in initial Ni(II) concentration. Variation of Ni(II) concentration from 10 to 70 mg L^{-1} resulted in a decrease of the rate coefficient from 0.095 to 0.015 min^{-1} (r ~ −0.93 to −0.98) (experimental conditions: adsorbent 5.0 g L^{-1}, Ni (II) 10–70 mg L^{-1}, pH 5.0, stirring speed 150 rpm, and temperature 298 K).

3.1.11. Zinc

Lin and Juang [125] have found that montmorillonite modified with sodium dodecylsulfate takes up Zn(II) from solution in a fast interaction such that the adsorption equilibrium was attained within 120 min (experimental conditions: adsorbent 2.0 g L^{-1}, Zn(II) 0.77 mM, and temperature 298 K).

Gupta and Sharma [9] have reported that Zn(II) adsorbs very slowly on bagasse Fly ash (a sugar industry waste) and needs 6 to 8 h to reach equilibrium although ~60% adsorption is over within 60 min. The first order rate coefficient has a value of 8.73×10^{-3} min^{-1} (experimental conditions: Zn(II) 1.22×10^{-3} to 3.06×10^{-3} M, fly ash 10.0 g L^{-1}, particle size 150–200 mesh, and temperature 303 K). The same group of authors also reported the adsorption of Zn(II) on red mud with rate constant of 2.14×10^{-3} min^{-1} (experimental conditions: adsorbent 10.0 g L^{-1}, Zn(II) 1.84×10^{-3} M, and pH 5.0) [113].

Zn(II) adsorption on fly ash (FA) and impregnated fly ash [with 0.1 M $Al(NO_3)_3$; IFA-Al and 0.1 M $Fe(Cl)_3$; IFA-Fe] [134] in the temperature range of 303 to 333 K, yielded first order rate coefficients of 0.104 to 0.184 min^{-1}, 0.108 to 0.196 min^{-1} and 0.120 to 0.214 min^{-1} for FA, IFA-Al and IFA-Fe, respectively (experimental conditions: adsorbent 1.42 g L^{-1}, Zn(II) 20 mg L^{-1}, pH 6.5, and stirring speed 100 rpm).

Similar is the case with adsorption of Zn(II) on silico-antimonate [114] with the first order rate coefficient having a value of 2.88×10^{-2} min^{-1} (experimental conditions: adsorbent 5.0 g L^{-1}, Zn(II) 50 mg L^{-1}, pH 4.0, and temperature 298 ± 1 K). First order kinetics was also proposed for adsorption of Zn(II) on iron(III) titanate [115] (with an equilibrium time of 180 min. The experimental data fitted Lagergren equation in agreement with the first order kinetics (experimental conditions: adsorbent 10.0 g L^{-1}, metal ions 50 mg L^{-1}, pH 4.15, and temperature 298 ± 1 K).

In a recent report, it has been shown that Zn(II) uptake by a powdered marble waste requires twice as much time (240 min) to attain equilibrium [137]. The first order rate coefficient in this case has a value of 0.038 min^{-1} (experimental conditions: adsorbent 2.0 g L^{-1}, Zn (II) 100 mg L^{-1}, pH 7.0, stirring speed 650 rpm, and temperature 298 K). For adsorption of Zn(II) on beach sand, the first order rate coefficient is much larger (0.11 ± 0.01 min^{-1}; r ~ 0.98) (experimental conditions: adsorbent 26.67 g L^{-1}, Zn(II) 9.17×10^{-5} M, particle size 300 μm, stirring speed 150 rpm, and temperature 303 ± 2 K) [138].

Similarly, the uptake of Zn(II) on pit coal fly ash [128] has been described as following first order kinetics with the rate coefficient increasing from 8.06×10^{-3} min^{-1} to 10.15×10^{-3} min^{-1} (r ~ 0.99) for initial concentration of Zn(II) varying from 30 to 100 mg L^{-1} (experimental conditions: adsorbent 10.0 g L^{-1}, and pH 4.5).

3.2. Second order kinetics

Equally large number of works has been reported where the second order kinetic model has been found to be the most suitable one for explaining adsorption of metal ions on inorganic solids. A collection of typical recent works is presented in Table 2 (Appendix) and the results are briefly discussed below.

3.2.1. Arsenic

In an earlier work, adsorption of As(III) and As(V) (as arsenite and arsenate anions respectively) on polymetallic sea nodules (composition: MnO_2 31.8%, Fe_2O_3 21.2%, and SiO_2 14.2% with traces of Cu, Ni, Co, Ca, K, Na and Mg) in aqueous medium was also shown to be following second-order kinetics with the rate coefficient of 18.47 (As (III)) and 12.32 g min^{-1} mg^{-1} (As(V)) [139]. Adsorption of As(III) and As(V) on a number of natural iron oxides (hematite, magnetite, and goethite) reached equilibrium within 2 days [140]. The second order rate coefficient for As(III) ranged from 0.52 ± 0.01 to 1.00 ± 0.01 m^2 mol^{-1} h^{-1} whereas the rate coefficient for As(V) adsorption varied from 0.44 ± 0.02 to 0.46 ± 0.02 m^2 mol^{-1} h^{-1}. Thus, As(V) was taken up at almost equal rates by the three iron oxide materials, but As(III) uptake rate differed with hematite showing lower rate. The second order model was interpreted as an example of chemical adsorption involving valence forces through sharing or exchange of

electrons between adsorbent and metal ions (experimental conditions: adsorbent 0.1 g L^{-1}, particle size 0.25 mm for hematite and goethite, and 0.1 mm for magnetite, and As(V) and As(III) 2×10^{-5} mol L^{-1}).

Adsorption of As(V) as arsenate anions on natural laterite [141] with variation of process parameters like As(V) concentration, temperature and ionic strength, has been proposed to follow second order kinetics. The basis for this is the good agreement between the amounts of As(V) adsorbed per unit mass (q_e) obtained from second-order model and the experimental equilibrium adsorption capacity (q_e). The second order rate coefficient increased with decreasing initial As(V) concentration. When As(V) concentration was low, adsorption was very fast due to easy availability of the active sites and less competition. With increasing As(V) concentration, competition for the adsorption sites became fierce and the adsorption rate fell down decreasing the rate coefficient. With an increase in adsorption temperature from 283 to 315 K, the rate processes continued to follow second order and the rate coefficient increased from 0.011 to 0.018 g mg^{-1} min^{-1} (initial As(V) 10.0 mg L^{-1}). The slight increase in the adsorption rate at higher temperature was shown to be due to the increasing mobility of As(V) ions in both the bulk of the solution and inside the pores. Second order kinetics was maintained even with increasing ionic strength. The authors have proposed that the surface of natural laterite becomes negatively charged due to accumulation of As(V) anions and this is balanced by Na^+ cations in solution leading to enhanced As(V) anion uptake at higher ionic strength (experimental conditions: As(V) 1 to 20 mg L^{-1}, ionic strength of NaCl 0.01 to 0.1 mol L^{-1}, stirring speed 2200 rpm, and temperature 283 to 315 K).

In another recent work, Yu et al. [142] proposed a second order mechanism for adsorption of As(V) on mesoporous alumina and activated alumina. The adsorption was rapid in the first 30 min for activated alumina and 100 min for mesoporous alumina and then approached equilibrium at ~300 min. The second order rate coefficients were 2.4×10^{-3} g min^{-1} mg^{-1} (mesoporous alumina) and 5.3×10^{-3} g min^{-1} mg^{-1} (activated alumina) (r ~ 0.99) (experimental conditions: adsorbent 0.4 g L^{-1}, As(V) 10 mg L^{-1}, and stirring speed 200 rpm). Activated alumina had a rate coefficient 2.2 times larger than that of mesoporous alumina, while the adsorption capacity of mesoporous alumina was almost 2.8 times higher than that of activated alumina (q_e: 24.8 for mesoporous alumina and 9.0 for activated alumina). The initial adsorption rate, h (product of rate constant and adsorption capacity at equilibrium) of mesoporous alumina was of 1.5 mg g^{-1} min^{-1}, about 3.8 times faster than that of activated alumina (h: 0.4 mg g^{-1} min^{-1}).

Several hydrated ferric oxide (HFO)-loaded polymeric hybrid adsorbents with different HFO loadings also took up As(V) [143] in a second order mechanism. The rate coefficient was generally higher for the adsorbents with lower HFO loadings. The rate coefficient, k_2, varied from 1.10×10^{-3} g mg^{-1} min^{-1} (HFO loading as Fe mass%: 3.4) to 0.030×10^{-3} g mg^{-1} min^{-1} (HFO loading: 17.3). It is suggested that a higher loading of HFO blocks more pores and thereafter lowers the rate at which As(V) diffuses into the pores and gets adsorbed (experimental conditions: adsorbent 0.5 g L^{-1}, As(V) 50 mg L^{-1}, and temperature 298 K).

3.2.2. Cadmium

Mathialagan and Viraraghavan [144] used perlite for the uptake of Cd(II) from aqueous solution where the Cd(II)–perlite interactions followed second order kinetics and the process required 360 min to reach the equilibrium. The second-order rate coefficient was 3.67 g mg^{-1} h^{-1} (r ~ 0.97) (experimental conditions: adsorbent 8.0 g L^{-1}, pH 6.0, stirring sped 170 rpm, and temperature 295 ± 1 K). Adsorption of Cd(II) from aqueous solutions by two clays, montmorillonite K-10 and natural Brazilian bentonite NT-25 attained equilibrium within 60 min (initial concentration 50 mg L^{-1}) [145]. In the temperature range of 278 to 298 K, the rate constant for K-10 and NT-25 varied from 0.13 to 2.01 g mg^{-1} min^{-1} and 0.13 to 6.75 g mg^{-1} min^{-1}, respectively. The initial adsorption rates varied from 0.33 to 1.38 mg g^{-1} min^{-1} for K-10/Cd(II) and 1.26 to 54.4 mg g^{-1} min^{-1} for NT-25/Cd(II) (experimental conditions: Cd(II) 50 mg L^{-1}, adsorbent 16.6 g L^{-1}, and temperature 278 to 298 K).

Sen Gupta and Bhattacharyya [146,147] have similarly proposed a second order kinetic model for adsorption of Cd(II) on kaolinite, montmorillonite, poly(oxo zirconium) and tetrabutylammonium derivatives of both, and acid-activated kaolinite and montmorillonite. This model is based not only on better second order plots (Fig. 1) but also on very small deviations between the sets of q_e values obtained from these plots and those measured experimentally. The second order rate coefficient varied from 3.7×10^{-2} to 4.1×10^{-2} g mg^{-1} min^{-1} for kaolinite and its modified forms and 3.4×10^{-2} to 11.1×10^{-2} g mg^{-1} min^{-1} for montmorillonite and its modified forms. The acid-activation increased the rate, which was much more prominent in case of montmorillonite (experimental conditions: adsorbent 2.0 g L^{-1}, Cd(II) 50 mg L^{-1}, pH 5.5, and temperature 303 K).

The removal of Cd(II) by modified aluminum-pillared montmorillonite from aqueous solutions was very fast in first 30 min and the process attained equilibrium within 360 min [148]. The authors did not report any value for the kinetic parameters, but Cd(II)–clay interactions were shown to follow second order kinetics. The theoretically predicted values of equilibrium adsorption were found to be close to the experimental values (experimental conditions: adsorbent 2.0 g L^{-1}, Cd(II) 60 mg L^{-1}, pH 6.0, and temperature 298 K).

Adsorption of Cd(II) on unmodified and PVA-modified kaolinite clay were also found to fit the second order kinetic model [149]. With PVA-modified kaolinite, the rate coefficient decreased with both increasing temperature and initial metal ion concentration. However, no particular trend was observed in case of unmodified kaolinite. It is found that clay modification not only enhanced the adsorption capacity of the adsorbent for Cd(II), but also increased the initial adsorption rates, which was also the case with increasing initial Cd(II) concentration. While the unmodified kaolinite showed an increase in

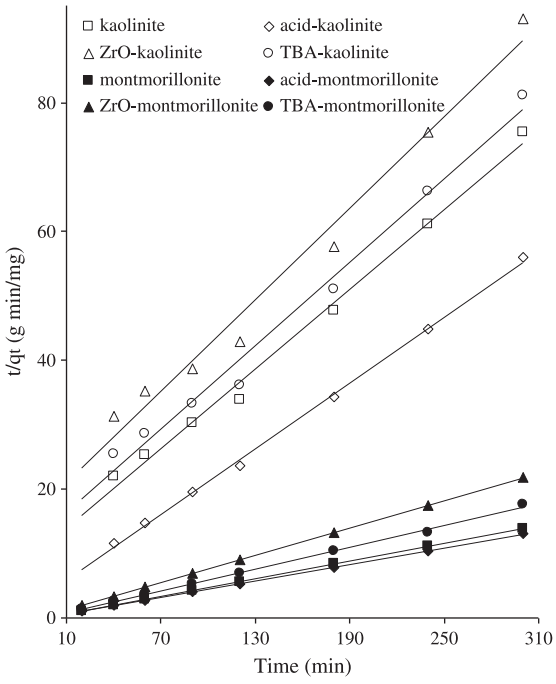

Fig. 1. Second order plots for Cd(II) adsorbed on natural and modified kaolinite and montmorillonite (experimental conditions: adsorbent 2 g L^{-1}, Cd(II) 50 mg L^{-1}, pH 5.5, and temperature 303 K).

the initial adsorption rates of Cd(II) with increasing temperature, modified kaolinite showed a reverse trend. It is possible that increasing temperature could have increased the mass transfer coefficients of Cd(II) towards the active sites on unmodified adsorbent, thereby reducing the time taken for the metal ions to interact with the active sites on the unmodified kaolinite surface (experimental conditions: kaolinite 15.0 g L^{-1} and PVA-modified kaolinite 5.0 g L^{-1}, stirring speed 150 rpm, temperature 298 to 323 K, and Cd(II) 300 to 1000 mg L^{-1} for kaolinite and 150 to 400 mg L^{-1} for PVA-modified kaolinite).

The use of Al_2O_3 for adsorption of Cd(II) by [150] had a second order rate coefficient influenced by varying initial metal ion concentration, pH, adsorbent dosage, and temperature. The initial metal ion concentration and adsorbent dosage had positive effect on the rate coefficient. The increase in solution temperature was shown to decrease the rate whereas higher solution pH resulted in a slight increase in the rate. The initial adsorption rate was enhanced by an increase in Cd(II) concentration (175.43 mg g^{-1} min^{-1} for Cd(II) 30 mg L^{-1} and 988.0 mg g^{-1} min^{-1} for Cd(II) 50 mg L^{-1}), adsorbent dose (151.51 mg g^{-1} min^{-1} for 10 mg Al_2O_3 and 175.43 mg g^{-1} min^{-1} for 30 mg Al_2O_3), pH (125.0 mg g^{-1} min^{-1} for pH 2.68 to 208.33 mg g^{-1} min^{-1} for pH 9.5) and was decreased by increasing the temperature (175.43 mg g^{-1} min^{-1} at 301.2 K to 136.98 mg g^{-1} min^{-1} at 333 K) (experimental conditions: adsorbent 2.0 and 6.0 g L^{-1}, Cd(II) 30 and 50 mg L^{-1}, pH 2.6, 6.7, 9.5, temperature 301.2, 313 and 333 K, and stirring speed 80 rpm). Second order kinetics was found to be the most favourable model for the removal of Cd(II) from aqueous solutions using clarified sludge from steel industry [151]. The rate coefficient was 1.606 g mg^{-1} min^{-1} (experimental conditions: adsorbent 7.5 g L^{-1}, Cd(II) 10 mg L^{-1}, pH 5.0, and temperature 303 ± 0.5).

Wu et al. [152] have also proposed second order kinetics for adsorption of Cd(II) on Fe- and Ca-montmorillonite with the Fe-clay having a higher rate coefficient (experimental conditions: adsorbent 4.0 g L^{-1}, Cd(II) 100 mg L^{-1}, pH 5.0, and temperature 298 K). Unuabonah et al. [153] have found that Cd(II) adsorption on sodium tetraborate-modified kaolinite increase with increasing temperature but decrease with increasing initial Cd(II) concentration. Thus, with initial Cd (II) concentration of 150 mg L^{-1}, the rate coefficient varied from 2.11×10^{-2} to 3.02×10^{-2} mg g^{-1} min^{-1} as the temperature changed from 298 to 323 K while the rate coefficient decreased from 2.11×10^{-2} to 1.21×10^{-3} mg g^{-1} min^{-1} for Cd(II) concentration increase from 150 to 400 mg L^{-1} at a fixed temperature of 298 K. It is proposed that increasing temperature results in breaking or thinning of the liquid film attached to the solid adsorbent particulates allowing the solute to reach the adsorbent surface with ease and therefore the rate coefficient increases with rising adsorption temperature (experimental conditions: adsorbent 5.0 g L^{-1}, Cd(II) 150, 300 and 400 mg L^{-1}, pH 5.5 ± 0.01, and temperature 298 to 323 K).

Panuccio et al. [154] from their work on adsorption of Cd(II) on zeolite, vermiculite and pumice have concluded that the process follow second order kinetics. For initial Cd(II) concentration range of 30 μM to 120 μM, the rate coefficient varied from 0.016 to 0.0061 g μg^{-1} day^{-1} on zeolite, 0.013 to 0.0073 g μg^{-1} day^{-1} on vermiculite and 0.0072 to 0.0061 g μg^{-1} day^{-1} on pumice (experimental conditions: adsorbent 10.0 g L^{-1}, Cd(II) 30 to 130 μm, stirring speed 30 rpm, and temperature 298 K). Adsorption of Cd(II) on loess soil from China also followed second order kinetics [155] (experimental conditions: adsorbent 10.0 g L^{-1}, Cd(II) 50 and 100 mg L^{-1}, and temperature 298 K).

Naiya et al. [156] also found recently that Cd(II) adsorption on activated alumina followed second order kinetics with the rate coefficient decreasing from 19.642×10^{-2} to 3.884×10^{-2} g mg^{-1} min^{-1} with increase in the initial Cd(II) concentration from 10 to 50 mg L^{-1}. In the same initial metal concentration range, the initial adsorption rate increased from 0.351 to 1.532 mg g^{-1} min^{-1} (experimental conditions: adsorbent 7.5 g L^{-1}, Cd(II) 10 to 50 mg L^{-1}, pH 5.0, and temperature 303 K).

Second order kinetics was also reported for adsorption of Cd(II) on thiol-functionalized silica from aqueous solution [157]. About 95% of Cd(II) were removed within 10 min and equilibrium was reached very quickly within 10–20 min. The fast adsorption rate was explained on the basis of easy access and availability of –SH groups which were the actual adsorption sites. The uniform microporous channels of the adsorbent also facilitated uptake of Cd(II) ions (pH 6.5 and temperature 298 K). For adsorption of Cd(II) on amino functionalized MCM-41 (NH_2-MCM-41), the second order rate coefficient showed a steady decrease with increase in initial Cd(II) concentration [136]. The values of k_2 varied from 0.502 to 0.005 g mg^{-1} min^{-1} for Cd(II) concentration of 10 to 70 mg L^{-1} (experimental conditions: adsorbent 5.0 g L^{-1}, Cd(II) 10–70 mg L^{-1}, pH 5.0, stirring speed 150 rpm, and temperature 298 K).

3.2.3. Chromium

Removal of anionic Cr(VI) by kaolinite and its modified forms (acid-activated kaolinite, ZrO-kaolinite, and TBA-kaolinite) yielded very good second order kinetic plots (Fig. 2) [158] and the values of q_e obtained from these plots were in close agreement with the values measured experimentally. The interactions therefore followed a second order mechanism and the rate coefficient values obtained from the plots varied between 3.6×10^{-2} to 6.8×10^{-2} g mg^{-1} min^{-1}. Acid-activated surface could attract Cr(VI) at a faster rate compared to untreated clay or ZrO- and TBA-modified forms and consequently, the acid activated kaolinite had a higher second order rate coefficient (experimental conditions: adsorbent 2.0 g L^{-1}, Cr(VI) as dichromate 50 mg L^{-1}, pH 4.6, and temperature 303 K). Adsorption of Cr(VI) from aqueous solution by Turkish vermiculite had also followed similar second order kinetics [159]. In this case, the removal efficiency increased gradually up to 85% with increasing contact time between 10 and 120 min and equilibrium was attained in 120 min. The rate coefficient showed a steady decrease from 0.35 g mg^{-1} min^{-1} to 0.15 g mg^{-1} min^{-1} as the temperature was increased from 293 K to 323 K (experimental conditions: adsorbent 10.0 g L^{-1}, Cr(VI) 25 mg L^{-1}, and pH 1.5)

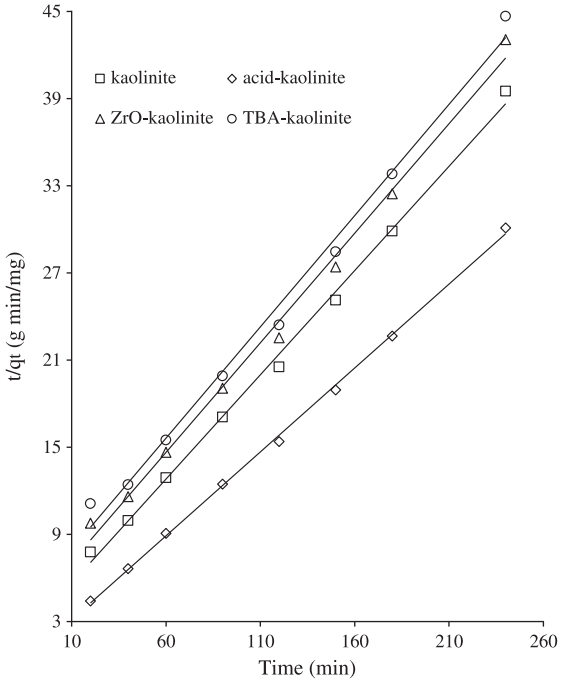

Fig. 2. Second order plots for Cr(VI) adsorbed on natural and modified kaolinite (experimental conditions: adsorbent 2 g L^{-1}, Cr(VI) 50 mg L^{-1}, pH 4.6, and temperature 303 K).

indicating an exothermic nature of the interactions. The authors demonstrated equivalence between theoretically computed and experimental values of the adsorption capacities.

Adsorption of both Cr(III) and Cr(VI) from aqueous solution on synthetic crystalline hydrous Ti(IV) oxide conformed to a second order mechanism [160] where the rate coefficient decreased with increasing solute concentration (experimental conditions: adsorbent 2.0 g L^{-1}, Cr (III) and Cr(VI) 10 mg L^{-1} and 20 mg L^{-1}, pH 5.0, for Cr(III) and 1.5 for Cr(VI), and temperature 303 K). Low-cost adsorbents like clarified sludge, activated alumina, Fuller's earth and fly ash were also seen to take up Cr(VI) with second order kinetics [161], the second order rate coefficient being in the range of 0.0534 mg g^{-1} min^{-1} (clarified sludge) to 0.1301 mg g^{-1} min^{-1} (fly ash) (experimental conditions: adsorbent 10.0 g L^{-1}, Cr(VI) 50 mg L^{-1}, pH 3.0, and temperature 303 ± 2 K).

In a comparative analysis of the second order kinetics for magnetite supported on montmorillonite (prepared by introducing magnetite nanoparticles), commercial micron-scale magnetite, and the parent magnetite for adsorption of Cr(VI) from water [162], it is observed recently that the parent magnetite has the highest second order rate coefficient. It is likely that the modification of magnetite has removed or blocked some of the adsorption sites that have highest affinity towards anionic Cr(VI) and as a result, the interactions take place with a reduced rate coefficient (experimental conditions: adsorbent 5.0 g L^{-1}, Cr(VI) 50 mg L^{-1}, stirring speed 160 rpm, and temperature 298 ± 2 K). In a similar work [163], Cr(VI) adsorption on nanoparticles of magnetite has been observed to possess a higher second order rate coefficient than diatomite-supported magnetite (experimental conditions: adsorbent 5.0 g L^{-1}, stirring speed 160 rpm, and temperature 298 ± 2 K). In another recent work, second order kinetics has been found more suitable for adsorption of Cr(VI) on hydrous zirconium oxide ($ZrO_2 \cdot nH_2O$) [164]. The interactions were very rapid and ~90% adsorption could be achieved in 45 min for Cr(VI) concentration of 100 mg L^{-1} (experimental conditions: adsorbent 2.0 g L^{-1}, Cr(VI) 100 and 200 mg L^{-1}, pH 2.0, and temperature 298 K).

3.2.4. Cobalt

It was observed that adsorption of Co(II) on kaolinite, montmorillonite and their acid-activated forms [165], ZrO-treated forms [166] and TBA-treated forms [167] obeyed second order kinetics. The second order plots are shown in Fig. 3 which yielded second order rate coefficient of 1.6×10^{-2} to 5.4×10^{-2} g mg^{-1} min^{-1}. The rate constant did not differ too much from natural to modified forms (experimental conditions: clay 2.0 g L^{-1}, Co(II) 50 mg L^{-1}, pH 5.8, and temperature 303 K). The uptake of Co(II) on treated bentonite was also reported with second order kinetics [168]. The rate coefficient decreased from 1.06×10^{-2} to 0.21×10^{-2} g mg^{-1} min^{-1} as the initial Co(II) concentration increased from 25 to 100 mg L^{-1}. Thus, increasing initial concentration and surface loading result in less diffusion efficiency and higher competition between metal ions for the fixed number of adsorption sites, consequently lower values of the rate coefficient were observed (experimental conditions: adsorbent 2.0 g L^{-1}, Co(II) 25 to 100 mg L^{-1}, temperature 303 K, and stirring speed 200 rpm).

3.2.5. Copper

Adsorption of Cu(II) on natural kaolinite attained equilibrium within 60 min [169]. The second order rate coefficient increased from 0.2384 g mg^{-1} min^{-1} to 0.3993 g mg^{-1} min^{-1} with increase in the temperature from 293 to 313 K (experimental conditions: adsorbent 2.0 g L^{-1}, Cu(II) 40 mg L^{-1}, and pH 6.0). Uptake of Cu(II) on kaolinite, montmorillonite, ZrO-kaolinite, ZrO-montmorillonite, TBA-kaolinite, TBA-montmorillonite [170], acid-activated kaolinite and acid-activated montmorillonite [171] has been found to be in conformity with second order kinetics. The second order plots are shown in Fig. 4 and the values of the rate coefficient obtained from these plots varied in the range of 9.4×10^{-2} to 14.4×10^{-2} g mg^{-1} min^{-1} for natural and

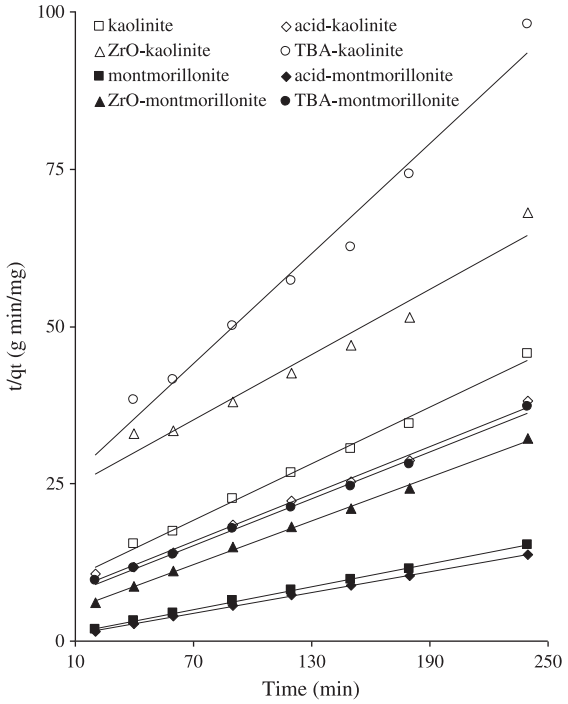

Fig. 3. Second order plots for Co(II) adsorbed on natural and modified kaolinite and montmorillonite (experimental conditions: adsorbent 2 g L^{-1}, Co(VI) 50 mg L^{-1}, pH 5.8, and temperature 303 K).

modified kaolinite and 7.7×10^{-2} to 15.8×10^{-2} g mg^{-1} min^{-1} for natural and modified montmorillonite (r ~ + 0.99) (experimental conditions: clay 2.0 g L^{-1}, Cu(II) 50 mg L^{-1}, pH 5.7, and temperature 303 K).

Cu(II) removal onto spent activated clay, following second order kinetics [172], had the rate of adsorption increasing with decreasing

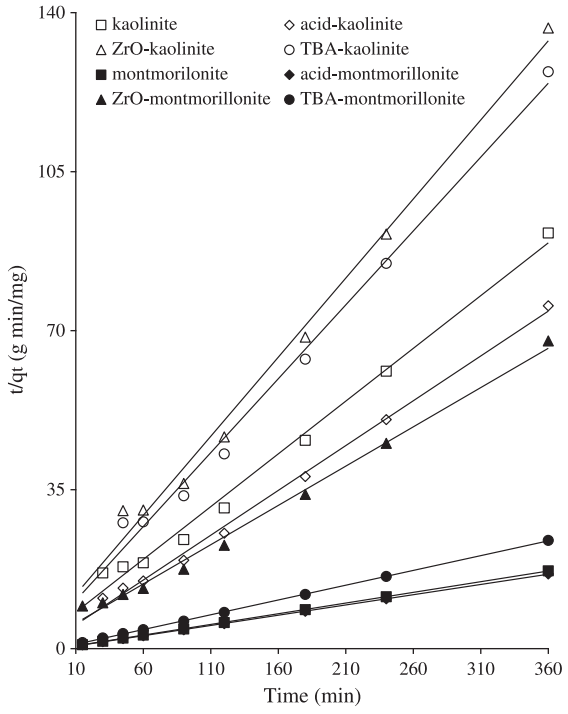

Fig. 4. Second order plots for Cu(II) adsorbed on natural and modified kaolinite and montmorillonite (experimental conditions: adsorbent 2 g L^{-1}, Cu(II) 50 mg L^{-1}, pH 5.7, and temperature 303 K).

initial solute concentration. The rate coefficient was inversely proportional to initial Cu(II) concentration and it was suggested that a higher Cu(II) loading would result in slower diffusion and stiff competition for the adsorption sites decreasing the rate coefficient (experimental conditions: clay 2.0 g L^{-1}, Cu(II) 1.907 mg L^{-1}, $NaClO_4$ 1×10^{-2} M, pH 5.0 ± 1, stirring speed 300 rpm, and temperature 300 K).

Kinetic studies for Cu(II) adsorption have also been reported with various organically treated clays. Thus, bentonite clay treated with 2,2′-dipyridyl has been recently modeled as a successful adsorbent for Cu(II) in aqueous solution [173], the interactions closely resembling second order kinetics. The second order rate coefficient increased from 4.89×10^{-2} g mg^{-1} min^{-1} to 9.28×10^{-2} g mg^{-1} min^{-1} when the temperature was raised from 293 to 323 K (initial Cu(II) 100 mg L^{-1}); whereas the rate coefficient varied from 4.89×10^{-2} g mg^{-1} min^{-1} to 1.99×10^{-2} g mg^{-1} min^{-1} in the initial Cu(II) concentration range of 100 to 200 mg L^{-1} at 293 K (experimental conditions: Cu(II) 100 mg L^{-1}, pH 5.7, and temperature 298 to 323 K). Another work on the kinetics of Cu(II) adsorption on silica gel with aminopropyl loading (1.01 mmol g^{-1}) by Manu et al. [174], was also best explained by a second order kinetic model. The rate coefficient increased with decrease in the initial Cu(II) concentration (experimental conditions: adsorbent 2.0 g L^{-1}, Cu (II) 65 and 1018 mg L^{-1}, pH 5.0, and temperature 303 ± 2 K). Removal of Cu(II) on bentonite treated with humic acid-immobilized-amine modified polyacrylamide also followed second order kinetics [168]. As the initial Cu(II) concentration increased from 25 to 100 mg L^{-1}, the rate coefficient decreased from 6.83×10^{-2} to 0.39×10^{-2} g mg^{-1} min^{-1} (experimental conditions: adsorbent 2.0 g L^{-1}, Cu(II) 25 to 100 mg L^{-1}, stirring speed 200 rpm, and temperature 303 K).

3.2.6. Iron

Very few works have been reported on Fe(II) and Fe(III) adsorption on inorganic materials and consequently, kinetics of adsorption of Fe has received little attention. One notable work on removal of Fe(III) by adsorption on kaolinite, montmorillonite and their modified forms (acid-activated, tetrabutylammonium and poly(oxo zirconium) derivatives) has shown the processed as following second order kinetics [166,167,175]. Interestingly, acid activation increased the second order rate coefficient marginally for montmorillonite (7.0×10^{-2} to 7.2×10^{-2} g mg^{-1} min^{-1}), but the influence was more prominent for kaolinite (4.7×10^{-2} to 7.4×10^{-2} g mg^{-1} min^{-1}). The other modified forms had a rate coefficient lower than that for the parent clays, although TBA-kaolinite possessed a higher value in comparison to natural kaolinite. The second order plots have almost perfect linearity (correlation coefficient ~ + 0.99) (Fig. 5) (experimental conditions: clay 2.0 g L^{-1}, Fe(III) 50 mg L^{-1}, pH 3.0, and temperature 303 K).

3.2.7. Lead

An interaction time of 120 min was required to attain equilibrium by natural clinoptilolite for the adsorption of Pb(II) from aqueous solution [176]. The second order kinetics was studied by changing the initial concentration of Pb(II), stirring speed and particle size. The rate coefficient showed a positive effect for the change of initial concentration of metal ions as well as of stirring speed. k_2 values varied from 64.53×10^{-3} to 159.20×10^{-3} g mg^{-1} min^{-1} (Pb(II) 10 to 100 mg L^{-1}) and 9.12×10^{-3} to 263.6×10^{-3} g mg^{-1} min^{-1} (stirring speed 100 to 225 rpm). However, the rate coefficient decreased from 130.40×10^{-3} to 113.03×10^{-3} g mg^{-1} min^{-1} for an increase in the particle size from 315–500 to 1000–1600 mm. The initial adsorption rate varied from 0.0853 to 15.698 mg g^{-1} min^{-1}, 0.0168 to 0.3735 mg g^{-1} min^{-1} and 0.1698 to 0.1250 mg g^{-1} min^{-1} respectively for the variation of Pb(II) concentration, stirring speed and particle size of the adsorbent (experimental conditions: adsorbent 10.0 mg L^{-1} and temperature 293 K).

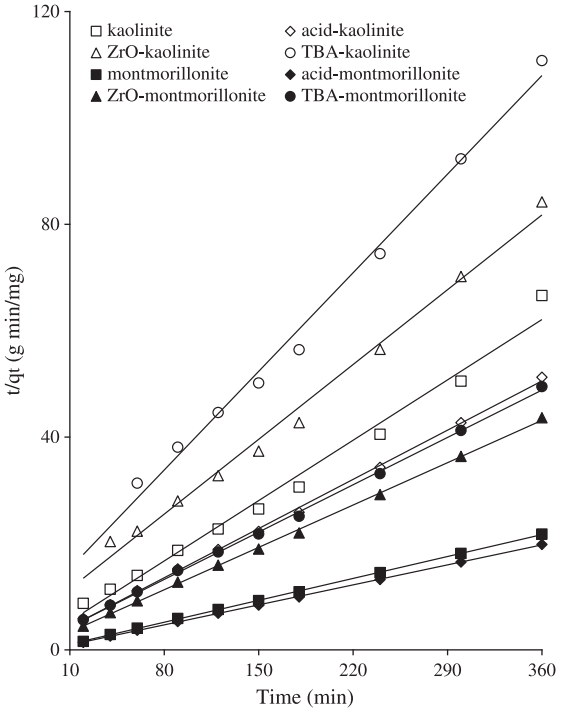

Fig. 5. Second order plots for Fe(III) adsorbed on natural and modified kaolinite and montmorillonite at 303 K (experimental conditions: adsorbent 2 g L^{-1}, Fe(III) 50 mg L^{-1}, pH 3.0, and temperature 303 K).

Natural kaolinite, montmorillonite and their modified forms (modified with ZrO-, TBA- and 0.25 M H_2SO_4) were also shown to be effective for removal of Pb(II) from aqueous solution [177,178] All the interactions fitted the second order kinetics model and the rate coefficient varied from 2.1×10^{-2} to 4.1×10^{-2} g mg^{-1} min^{-1} for kaolinite and its derivatives and from 6.4×10^{-2} to 11.2×10^{-2} g mg^{-1} min^{-1} for montmorillonite and its derivatives. The second order kinetic plots are shown in Fig. 6. It has been observed that the rate coefficient for montmorillonite was about 2.5 times the corresponding value for kaolinite even without treatment. Acid activation raised the second order rate coefficient marginally for kaolinite (3.5×10^{-2} to 4.1×10^{-2} g mg^{-1} min^{-1}), but the influence was much prominent for montmorillonite (8.4×10^{-2} to 11.2×10^{-2} g mg^{-1} min^{-1} after acid activation) (experimental conditions: clay 2.0 g L^{-1}, Pb(II) 50 mg L^{-1}, pH 5.7, and temperature 303 K).

The kinetics of Pb(II) adsorption on Turkish kaolinite was studied at different temperatures [179] and it was found that the rate coefficient decreased from 8.38×10^{-2} to 4.33×10^{-2} g mg^{-1} min^{-1} as the temperature was raised from 293 to 323 K (experimental conditions: adsorbent 0.1 g, Pb(II) 10 mg L^{-1}, and pH 5.0). The use of activated alumina-supported iron oxide for uptake of Pb(II) from aqueous solution was [180] characterized by an increase in the adsorption rate considerably in the first 2 h for various initial concentrations, and equilibrium was reached gradually at about 4, 8, 12 and 36 h corresponding to Pb(II) initial concentrations of 0.1, 0.2, 0.4 and 0.8 mM, respectively. The kinetics revealed second order mechanism with the rate coefficient decreasing from 0.1999 to 0.0061 g mg^{-1} h^{-1} as the initial concentration of Pb(II) was changed from 0.1 to 0.8 mM and the amount of Pb(II) adsorbed (q_e) increasing from 4.28 to 31.51 mg g^{-1}. These values were found very close to experimental q_e values (experimental conditions: adsorbent 5.0 g L^{-1}, pH 5.0, stirring speed 150 rpm, and temperature 300 ± 1 K).

Interactions of Pb(II) ions with natural montmorillonite were found to attain equilibrium within 100 min [181]. The second order rate coefficient was 3.84×10^{-3} g mg^{-1} min^{-1}. The initial uptake was very rapid with a rate of 9.79 mg g^{-1} min^{-1}, before increased

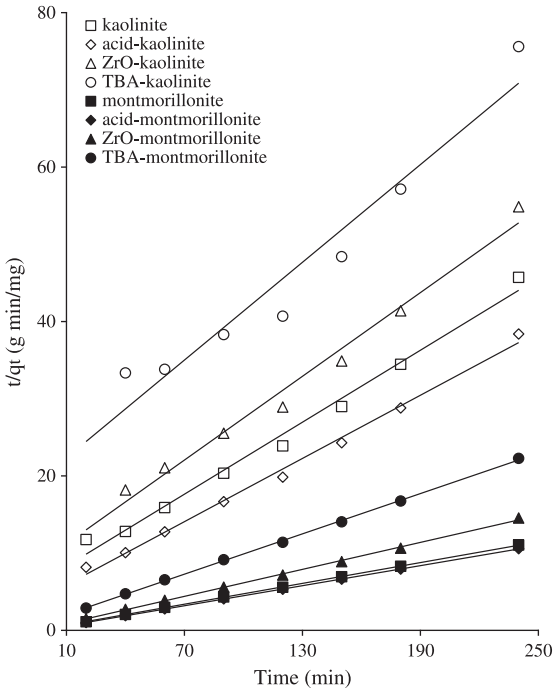

Fig. 6. Second order plots for Pb(II) adsorbed on natural and modified kaolinite and montmorillonite (experimental conditions: adsorbent 2 g L^{-1}, Pb(II) 50 mg L^{-1}, pH 5.7, and temperature 303 K).

coverage decreased the rate (experimental conditions: Pb(II) 150 mg L^{-1}, pH 6.0, stirring speed 160 rpm, and temperature 298 K).

Removal of Pb(II) on clay–poly(methoxyethyl)acrylamide [182] followed second order kinetic model and the rate coefficient increased from 1.70×10^{-2} g mg^{-1} min^{-1} to 2.91×10^{-2} g mg^{-1} min^{-1} for an increase in solution temperature from 293 K to 323 K. The values of Δq (%) for the best-fit second order model, remained between 1.607% and 2.694% (experimental conditions: adsorbent 2.0 g L^{-1}, Pb(II) 100 mg L^{-1}, stirring speed 200 rpm, and temperature 293 to 323 K).

Adsorption data for Pb(II) on unmodified and PVA-modified kaolinite clay also fit the second order kinetic model [149]. For the unmodified kaolinite, the rate coefficient increased with temperature and decreased with increase in initial Pb(II) concentration. With PVA-modified kaolinite the rate decreased with both increasing temperature and initial Pb(II) concentration. The initial adsorption rates for unmodified kaolinite were comparatively lower than those of the modified clay, indicating that the clay modification enhanced both Pb (II) adsorption capacity and the rate of adsorption. For the unmodified kaolinite, the adsorption rate increased with increasing temperature, but the modified kaolinite showed a reverse trend. It was suggested that at a higher temperature. the mass transfer coefficient of Pb(II) towards the active sites would increase with respect to the unmodified adsorbent, thereby reducing the time taken by the metal ions to interact whereas such a situation would not develop for the modified adsorbent (experimental conditions: kaolinite 15.0 g L^{-1} and PVA-modified kaolinite 5.0 g L^{-1}, stirring speed 150 rpm, temperature 298 to 323 K, and Pb(II) 300 to 1000 mg L^{-1} for kaolinite and 150 to 400 mg L^{-1} for PVA-modified kaolinite).

Pb(II) removal by natural mordenite [183] has been suggested to follow second order kinetics. The solution temperature had a positive influence on the reaction rate, which increased from 0.0071 to 0.0094 g mg^{-1} min^{-1} in the temperature interval of 293 to 313 K (experimental conditions: adsorbent 2.0 g L^{-1}, Pb(II) 40 mg L^{-1}, pH 6.0, stirring speed 150 rpm, and temperature 293 to 313 K).

The second order process of Pb(II)–bentonite interactions in aqueous solution [184] had a rate coefficient of 0.024 g mg^{-1} h^{-1} (experimental conditions: Pb(II) 4.83×10^{-5} mol L^{-1}, pH 4.2 ± 0.1, and temperature 293.15 K). Unuabonah et al. [153] have also reported second order adsorption of Pb(II) on sodium tetraborate-modified kaolinite where the rate coefficient increased with increasing temperature but decreased with increasing initial Pb(II) concentration. The rate coefficient varied from 1.19×10^{-2} to 2.66×10^{-2} mg g^{-1} min^{-1} as the temperature changed from 298 to 323 K (Pb(II) 150 mg L^{-1}) and from 1.19×10^{-2} to 1.07×10^{-3} mg g^{-1} min^{-1} as the initial Pb(II) concentration increased from 150 to 400 mg L^{-1} (at 298 K). The reason for the affect of temperature was suggested as the break-up of the liquid film surrounding the solid particulates at a higher temperature exposing the bare surface to Pb(II) cations. The initial adsorption rate increased for both increasing Pb(II) concentration and increasing temperature (experimental conditions: adsorbent 5.0 g L^{-1}, Pb(II) 150, 300 and 400 mg L^{-1}, pH 5.5 ± 0.01, and temperature 298 to 323 K).

Bentonite treated with 8-hydroxy quinoline also showed a similar behaviour with respect to Pb(II) adsorption [60]. By increasing the solution temperature from 293 K to 323 K, the second order rate coefficient increased from 7.37×10^{-3} g mg^{-1} min^{-1} to 2.36×10^{-2} g mg^{-1} min^{-1} with an initial Pb(II) concentration of 112.5 mg L^{-1}. Moreover, for a fixed temperature of 293 K, the rate coefficient decreased from 1.29×10^{-2} to 5.77×10^{-3} g mg^{-1} min^{-1} for initial Pb(II) concentration increasing from 100 mg L^{-1} to 150 mg L^{-1} (experimental conditions: Pb(II) 100 mg L^{-1}, pH 5.5, and temperature 293 to 313 K).

Adsorption of Pb(II) from water on palygorskite was reported by Fan et al. [185] with a second order rate coefficient of 0.089 g mg^{-1} h^{-1}. The uptake was very fast and reached equilibrium within 180 min (experimental conditions: adsorbent 0.4 g L^{-1}, Pb(II) 6.76×10^{-5} mol L^{-1}, pH 5.5 ± 0.2, and temperature 293 ± 2 K).

Liang et al. [157] have found that uptake of Pb(II) by thiol-functionalized silica was very rapid and ~95% of Pb(II) were removed within 10 min. The fast adsorption rate suggested that the –SH groups were readily available and easily accessible to Pb(II) because of the uniform microporous channels of the adsorbent. Another adsorbent, amino functionalized MCM-41 (NH_2-MCM-41) was also found to adsorb Pb(II) from aqueous solution [135] through a second order process where the rate coefficient decreased with the increase in initial Pb(II) concentration. Variation of Pb(II) concentration from 10 to 70 mg L^{-1} was accompanied by a change in the rate coefficient from 14.861 to 0.181 g mg^{-1} min^{-1} (experimental conditions: adsorbent 5.0 g L^{-1}, Pb(II) 10 to 70 mg L^{-1}, pH 5.0, stirring speed 150 rpm, and temperature 298 K).

When activated alumina was used as the adsorbent for Pb(II) [156], the kinetics were also found to be of second order and the rate coefficient decreased from 12.27×10^{-2} to 2.34×10^{-2} g mg^{-1} min^{-1} for Pb(II) concentration increasing from 10 to 50 mg L^{-1}. In the same concentration range, the initial adsorption rate increased from 0.496 to 2.044 mg g^{-1} min^{-1}. Thus, with a bare surface, more Pb(II) cations got bound to alumina surface immediately, but as the surface coverage increased, the rate of uptake came down when large number of Pb(II) cations are competing with one another for the adsorption sites (experimental conditions: adsorbent 7.5 g L^{-1}, Pb(II) 10 to 50 mg L^{-1}, pH 5.0, and temperature 303 K). Binding of Pb(II) to a montmorillonite–illite type of clay [186] also showed a similar decrease in the second order rate coefficient from 0.1097 to 0.0022 g mg^{-1} min^{-1} for Pb (II) concentration increasing from 100 to 200 mg L^{-1} (experimental conditions: adsorbent 2.5 g L^{-1}, Pb(II) 100 to 200 mg L^{-1}, pH 4.0, and temperature 310 K).

Second order kinetics has also been reported by Liu et al. [187] recently when steel slag is used for removing Pb(II) from water. The second order rate coefficient has the value of 13.26 g mg^{-1} min^{-1} (experimental conditions: adsorbent 30.0 g L^{-1}, particle size 0.18 to 0.125 mm, Pb(II) 100 mg L^{-1}, pH 5.0, and temperature 293 K).

3.2.8. Manganese

Not many works have been reported for adsorption of Mn(II) on inorganic solids. It was found that Mn(II) adsorbs on montmorillonite K-10 and natural Brazilian bentonite NT-25 with a second order mechanism and the equilibrium was attained very rapidly within 60 min (initial concentration 50 mg L^{-1}) [145]. In the temperature range of 278 to 298 K, the rate coefficient for K-10 varied from 0.41 to 2.51 g mg^{-1} min^{-1}, and the same for NT-25 from 0.18 to 0.64 g mg^{-1} min^{-1}. The initial adsorption rates of Mn(II) varied from 0.52 to 4.97 mg g^{-1} min^{-1}, 1.57 to 10.1 mg g^{-1} min^{-1} for K-10 and NT-25 respectively (experimental conditions: adsorbent 16.6 g L^{-1}, Mn(II) 50 mg L^{-1}, and temperature 278 to 298 K).

3.2.9. Nickel

In several works, Ni(II) adsorption on clays and other inorganic adsorbents has been shown to closely resemble second order kinetics. Bhattacharyya and Sen Gupta [188] reported the second order kinetics as the most suitable model for Ni(II) adsorption on natural and modified (with ZrO- and TBA-) kaolinite and montmorillonite. It was also the case with acid activated kaolinite and montmorillonite [189]. The second order rate coefficient for kaolinite, montmorillonite and their modified forms remained in a narrow range of values from 1.3×10^{-2} to 5.46×10^{-2} g mg^{-1} min^{-1}. Ni(II) uptake by acid-activated montmorillonite was the most rapid while TBA-kaolinite had the slowest uptake. For the clays and their modified forms, the second order plots (Fig. 7) had very good linearity and the q_e values given by these plots agreed very well with the experimentally determined equilibrium solid phase concentrations (experimental conditions: clay 2.0 g L^{-1}, Ni(II) 50 mg L^{-1}, pH 5.7, and temperature 303 K).

Another case of second order kinetics was reported for Ni(II) removal from aqueous solution by Mg-mesoporous alumina [190], the rate coefficient in this case decreased from 9.073 g mg^{-1} h^{-1} to 0.325 g mg^{-1} h^{-1} as the initial Ni(II) concentration was increased from 10 mg L^{-1} to 30 mg L^{-1} (experimental conditions: adsorbent 1.0 g L^{-1}, Ni(II) 10 to 30 mg L^{-1}, pH 4.8, stirring speed 150 rpm, and temperature 298 ± 1).

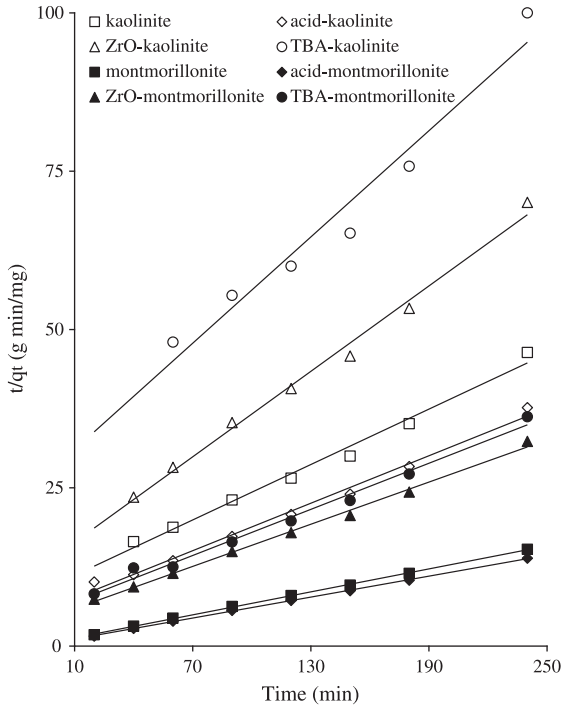

Fig. 7. Second order plots for Ni(II) adsorbed on natural and modified kaolinite and montmorillonite (experimental conditions: adsorbent 2 g L^{-1}, Ni(II) 50 mg L^{-1}, pH 5.7, and temperature 303 K).

The natural silicoaluminate, clinoptilolite, takes up Ni(II) from aqueous solution [191] with a second order rate coefficient of 0.522 g mg^{-1} min^{-1} to 1.2 g mg^{-1} min^{-1} corresponding to solution temperature of 293 to 333 K (experimental conditions: adsorbent 15.0 g L^{-1}, particle size 0.2 mm, Ni(II) 25 mg L^{-1}, pH 7, and stirring speed 250 rpm). When montmorillonite, K10, was modified with 3-mercapto-propyltrimethoxysilane, the new material adsorbs Ni(II) in a second order mechanism similarly to the parent montmorillonite [192]. Ni(II) uptake was shown to be a fast process in which equilibrium was attained within 5 and 15 min for the parent and the modified clay respectively. Incorporation of 3-mercapto-propyl-trimethoxysilane into montmorillonite has obviously slowed down the interactions with Ni(II) (experimental conditions: adsorbent 16.6 g L^{-1}, Ni(II) 100 mg L^{-1}, and temperature 298 K).

3.2.10. Selenium

Adsorption of Se(IV) in the form of the oxyanion, selenate (SeO_4^{2-}), on layered double hydroxide, LDH (Zn/Al and Mg/Al) with varying composition (M^{2+}:M^{3+} molar ratio = 3 and 2) was also found to have adsorption characteristics in conformity with second order kinetics [193]. M^{2+}:M^{3+} molar ratio of the LDH had significant influence on the rate of adsorption. It was found that the rate of Se(IV) adsorption on MACl-3 (Mg/Al/Cl LDH having M^{2+}:M^{3+} molar ratio = 3) was almost 12 to 18 times faster than that of the three other LDHs, MACl-2 (Mg/Al/Cl LDH with M^{2+}:M^{3+} molar ratio = 2), ZACl-3 (Zn/Al/Cl LDH with M^{2+}:M^{3+} molar ratio = 3) and ZACl-2 (Zn/Al/Cl LDH with M^{2+}:M^{3+} molar ratio = 2). The adsorption rates were in the order MACl-3>ZACl-3>MACl-2>ZACl-2 (experimental conditions: adsorbent 1.0 g L^{-1}, Se (IV) 50.34 mg L^{-1}, and temperature 298 K). Another work reporting adsorption of Se(IV) on TiO_2 also followed second order kinetics [194]. The adsorption rate coefficient varied with the concentration of Se(IV) oxy-anion and pH and it was observed that the rate coefficient decreased from 5351.0 to 14.0 g $mmol^{-1}$ h^{-1} and from 3318.0 to 2556.0 g $mmol^{-1}$ h^{-1}, for Si(IV) concentration of 5.90×10^{-6} to 5.89×10^{-4} mol L^{-1} and solution pH from 3.00 ± 0.05 to 8.00 ± 0.09, respectively (experimental conditions: adsorbent 5.0 g L^{-1}, Se(IV) 5.90×10^{-6} to 5.89×10^{-4} mol L^{-1}, pH 3.00 ± 0.05 to 8.00 ± 0.09, ionic strength 0.1 mol L^{-1}, and temperature 296 ± 2 K).

3.2.11. Zinc

Adsorption of Zn(II) on phosphogypsum followed the second order model with rate coefficient of 0.3217 g mg^{-1} min^{-1} [195] (experimental conditions: adsorbent 4.0 g L^{-1}, Zn(II) 50 mg L^{-1}, stirring speed 200 rpm). Smectite clay pillared with Al(III), Ti(IV) and ZrO– species interacted with Zn(II) ions showing better agreement with a second order mechanism [196]. The second order rate coefficient had values of 4.17 to 10.69 g mg^{-1} min^{-1} and 3.98 to 10.43 g mg^{-1} min^{-1} for two different sets of adsorbents prepared at two different calcination temperatures (experimental conditions: adsorbent 3.0 g L^{-1}, Zn(II) 50 mg L^{-1}, pH 5.0, and temperature 298 ± 1 K).

Kaolin clay has been found to be a good adsorbent for Zn(II) [197] and the interactions are best explained by second order kinetics that depend on the adsorbent amount, solution temperature, pH and Zn (II) concentration. The initial rate of adsorption was very fast that decreased from 77.52 to 42.02 mg g^{-1} min^{-1} for Zn(II) concentration of 30 to 50 mg L^{-1} and from 55.83 to 38.41 mg g^{-1} min^{-1} for 10 to 30 mg kaolin, increased from 2.33 to 67.12 mg g^{-1} min^{-1} in the pH range of 3.3 to 8.1 and from 55.83 to 107.71 mg g^{-1} min^{-1} in the temperature range of 303 to 338 K. In another work, Tang et al. [198] found the removal of Zn(II) from aqueous solution with natural Chinese loess soil to be of second order kinetics having a rate coefficient of 2.35×10^{-4} to 1.10×10^{-4} g mg^{-1} min^{-1} when the adsorption temperature was varied from 288 to 318 K (experimental

conditions: adsorbent 10.0 g L^{-1}, Zn(II) 500 mg L^{-1}, temperature 288 to 318 K, and stirring speed 180 rpm).

Anirudhan and Suchithra [168] used humic acid-immobilized polymer/bentonite composite as the adsorbent material to treat Zn (II)-contaminated water and observed that the interactions had a clear trend to follow a second order mechanism of adsorption. As Zn(II) concentration increased from 25 to 100 mg L^{-1}, the rate coefficient decreased from 2.56×10^{-2} to 0.28×10^{-2} g mg^{-1} min^{-1}. Increasing Zn(II) concentration reduces transport of the ions to the surface by diffusion, but enhances competition for adsorption sites, consequently the rate slows down (experimental conditions: adsorbent 2.0 g L^{-1}, Zn (II) 25 to 100 mg L^{-1}, temperature 303 K, and stirring speed 200 rpm).

Adsorption of Zn(II) on zeolites, NaA and NaX, has also been explained on the basis of a second order model [199]. The rate coefficient as well as the initial adsorption rate increased with the increase in temperature. Thus, by increasing the temperature from 298 to 323 K, the rate coefficient increased from 0.60×10^{-3} to 0.72×10^{-3} g mg^{-1} min^{-1} and the initial adsorption rate from 8.27 to 10.12 mg g^{-1} min^{-1} for Zn(II)–NaA interactions. Similar trend was observed in case of Zn(II)–NaX interactions (experimental conditions: Zn(II) 100 mg L^{-1}, pH 6.0, stirring speed 200 rpm, and temperature 298 to 323 K).

3.3. Elovich equation

Fitting of the experimental data to the Elovich equation has been tried only by a few authors. Some recent works along with the Elovich coefficients and the experimental conditions are summarized in Table 3 (Appendix). Cortés-Martínez et al. [200] have shown that the equation is fitted very well for adsorption of Cd(II) on natural clinoptilolite and hexadecyltrimethylammonium-clinoptilolite. The initial adsorption rate (Elovich α) had values of 72.36 mg g^{-1} and 295.36 mg g^{-1} on natural and modified clinoptilolite respectively. The desorption coefficient (Elovich β) was 0.427 mg^{-1} g and 0.575 mg^{-1} g on natural and modified clinoptilolite respectively.

Uptake of Pb(II) on montmorillonite [181] had α and β values of 1.49×10^{19} mg g^{-1} min^{-1} and 0.9841 mg g^{-1} respectively. The experimental data for adsorption of Pb(II) on natural mordenite were found similarly to produce good fit with the Elovich model [183]. The good fit provides additional support for a second order mechanism. The Elovich coefficients, α (g mg^{-1} min^2) and β (mg g^{-1} min^{-1}) were found to be temperature-dependent (293 K: α = 2.6899, β = 1.3507; 303 K: α = 2.6026, β = 2.8271; and 313 K: α = 2.6511, β = 12.8622). Adsorption of Zn(II) on smectite clay [196] pillared with Al (III), Ti(IV) and ZrO– species also yielded good Elovich plots that gave α and β in the ranges of 7.40×10^{-3} to 40.76×10^{-3} g $mmol^{-1}$ min^2 and 1.12 to 1.68 mmol g^{-1} min^{-1} respectively.

Debnath and Ghosh [160] applied Elovich equation for uptake of Cr (III) and Cr(VI) on hydrous TiO_2 at different initial metal ion concentrations. Interestingly, α increased at higher Cr(III) or Cr(VI) concentrations, but β had a reverse trend. The same group of authors have found the Elovich coefficients for adsorption of Ni(II) on TiO_2 [135] in the temperature range of 288 to 318 K and found that α varied from 2.45 to 13.35 (Ni(II) 10 mg L^{-1}), 4.89 to 49.27 (Ni(II) 30 mg L^{-1}) and 7.84 to 59.15 (Ni(II) 50 mg L^{-1}) and the corresponding values of β were in the range of 95.35×10^2 to 125.47×10^2, 30.11×10^2 to 43.23×10^2 and 17.54×10^2 to 25.59×10^2.

It may be noted that there is no consistency in the values of Elovich coefficients, reported by various authors and sometimes, apparently abnormal values are also found. For example, α varied from 7.36×10^{28} to 5.49×10^{70} mg g^{-1} min^{-1} and that of β from 1.784 to 3.974 mg g^{-1} for Cu(II) adsorption on bentonite clay treated with 2,2′-dipyridyl [173] in the temperature range 293 to 323 K. On the other hand, the experimental data for Cd(II) adsorption on Fe- and Ca-montmorillonite were shown to fit the Elovich model [152] without computation of the coefficients.

Kinetics of adsorption of Cd(II), Co(II), Cu(II), Fe(III), Pb(II) and Ni (II)) on kaolinite, montmorillonite, and their modified forms (treated with tetrabutylammonium bromide, zirconium oxychloride, 0.25 M sulphuric acid) and of anionic Cr(VI) on kaolinite and its modified forms (treated with tetrabutylammonium bromide, zirconium oxychloride, and 0.25 M sulphuric acid) was tested utilizing the Elovich equation as an alternative model of second order kinetics [158,165,171,175,178,188,201]. Typical results are shown in Figs. 8 and 9. The plots had good linearity in all the cases and the acid activated montmorillonite possessed the highest values of α for all the metal ions. The values show that α is directly correlated with the amount adsorbed per unit mass of clays (q_e). The values of β were lying in a narrow range for all clay–metal interactions.

3.4. Intra-particle diffusion

On porous adsorbents, pore diffusion or intra-particle diffusion is also likely to play a significant role along with surface adsorption. Many workers have thus studied pore diffusion on the basis of Eq. (13) to see whether intra-particle diffusion plays a role in determining the kinetics and hence the mechanism of adsorption. A collection of values of intra-particle diffusion coefficients obtained by various groups are summarized in Table 4 (Appendix).

The removal of Cu(II), Zn(II) [202] and Cr(III), Pb(II) [203] on bagasse fly ash obeyed particle diffusion mechanism particularly at comparatively higher concentration of the adsorbate. Adsorption of Ni (II) and Zn(II) on fly ash (FA) and impregnated fly ash (IFA-Al and IFA-Fe) [113] has already been shown to follow first order kinetics, but the process was also likely to have significant contribution from pore diffusion. In the temperature range of 303 to 333 K, the diffusion coefficient (k_{id}) for Ni(II) adsorption varied from 30.00×10^2 to 18.18×10^2 mg g^{-1} $min^{-0.5}$, 72.73×10^2 to 41.67×10^2 mg g^{-1} $min^{-0.5}$ and 57.14×10^2 to 40.00×10^2 mg g^{-1} $min^{-0.5}$ for FA, IFA-Al and IFA-Fe, respectively. k_{id} values for Zn(II) adsorption varied from 15.0×10^2 to 40.0×10^2 mg g^{-1} $min^{-0.5}$ for FA, 25.0×10^2 to 55.56×10^2 for IFA-Al and 33.0×10^2 to 75.0×10^2 for IFA-Fe. Rengaraj et al. [204] studied the

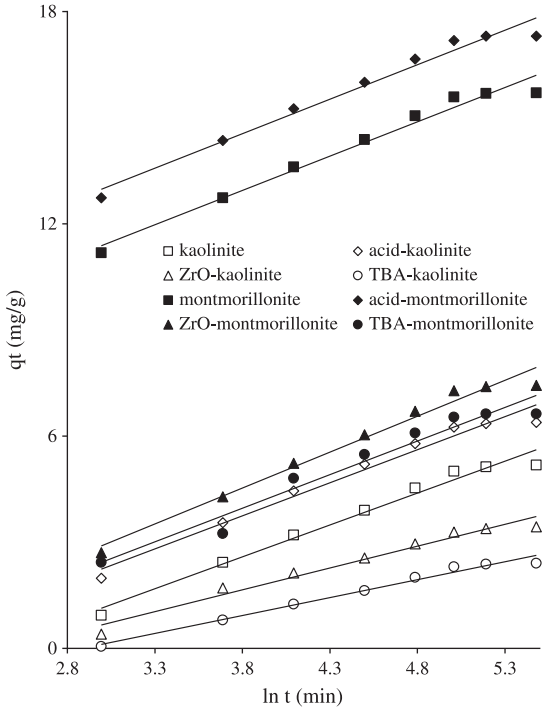

Fig. 8. Elovich plots for adsorption of Ni(II) on natural and modified kaolinite and montmorillonite (experimental conditions: adsorbent 2 g L^{-1}, Ni(II) 50 mg L^{-1}, pH 5.7, and temperature 303 K).

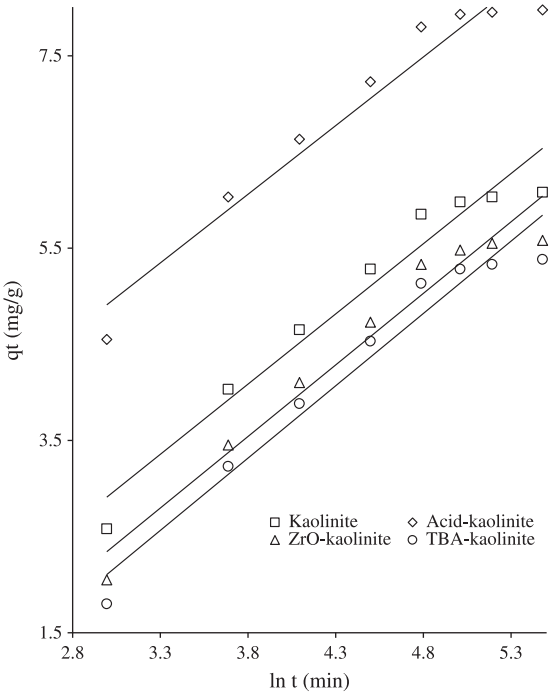

Fig. 9. Elovich plots for adsorption of Cr(VI) on natural and modified kaolinite (experimental condition: adsorbent 2 g L^{-1}, Cr(VI) 50 mg L^{-1}, and pH 4.6).

intra-particle diffusion plots for removal of Cu(II) by aminated and protonated mesoporous aluminas. The initial steep-sloped portion (from 0 to 1.5 h) was attributed to external surface adsorption or instantaneous adsorption, while the gentle-sloped portion (from 1.5 to 2.75 h) was attributed to intraparticle diffusion which was rather slow and was likely to be rate-controlled. By changing Cu(II) concentration from 10 to 20 mg L^{-1}, the rate coefficient varied from 1.0714 to 1.8957 mg g^{-1} $h^{-0.5}$ and 1.8484 to 3.4009 mg g^{-1} $h^{-0.5}$ respectively, for aminated and protonated alumina.

There are also cases reported in the literature where application of the Eq. (13) was studied under different experimental conditions. For example, Bektas and Kara [176] tried to apply the equation to adsorption of Pb(II) on natural clinoptilolite with varying stirring speed, initial Pb (II) concentration and particle size. Some of the plots had poor linearity (regression coefficient, r~0.48 to 0.91). The intra-particle diffusion coefficient had values of 0.075 to 0.005 mg g^{-1} min^{-1} (stirring speed 100 to 225 rpm), 0.0295 to 0.0152 mg g^{-1} min^{-1} (Pb(II): 10 to 100 mg L^{-1}), 0.0303 to 0.0270 mg g^{-1} min^{-1} (particle size 315–500 to 1000–1600 μm). These values indicate that intra-particle diffusion should have appreciable influence on the overall kinetics, but no conclusion was drawn by the authors.

Although adsorption of Cu(II) on kaolinite [169] followed second order kinetics, it was shown that intra-particle diffusion might also play some role. The qt vs. t1/2 plots were linear for about 10 min indicating diffusion of Cu(II) cations into the pores and then, reached a plateau corresponding to completion of pore diffusion. As in most other cases, the plots did not have zero intercept and therefore, the authors concluded that intra-particle diffusion was not the sole process governing the kinetics. The intra-particle diffusion coefficients were 0.6441 mg g^{-1} $min^{-0.5}$ at 293 K, 0.1859 mg g^{-1} $min^{-0.5}$ at 303 K and 0.3111 mg g^{-1} $min^{-0.5}$ at 313 K.

Pb(II) adsorption on Turkish kaolinite also demonstrated possibility of intra-particle diffusion [179] despite closely following second order kinetics. The pore diffusion rate coefficient decreased from 0.28 to 0.24 mg g^{-1} $min^{-0.5}$ when the temperature was increased from 293 to 323 K. However, the non-zero intercepts (0.89 to 0.46 mg g^{-1}in the temperature range of 293 to 323 K indicate that the kinetics cannot be explained on the basis of Eq. (13) alone.

Two-stage intra-particle diffusion has also been proposed by some other workers. For example, Huang et al. [121] have shown that adsorption of Cr(VI) on organic-modified rectorite (viz, dodecyl benzyl dimethyl ammonium rectorite, OREC1, hexadecyl trimethyl ammonium rectorite, OREC2, and octadecyl trimethyl ammonium rectorite, OREC3) could at least be partially explained on the basis of very fast pore diffusion to begin with and then, a slow diffusion process that filled up the pores. The two stages had two different diffusion rate coefficients, e.g., 0.272 and 0.00371 mg g^{-1} $min^{-0.5}$ for OREC1, 0.316 and 0.00898 mg g^{-1} $min^{-0.5}$ for OREC2 and 0.383 and 0.00965 mg g^{-1} $min^{-0.5}$ for OREC3. The overall kinetics was however shown to be pseudo first order. Taqvi et al. [138] similarly reported existence of intra-particle diffusion at least up to first 25 min within the first order kinetics for adsorption of Zn(II) on beach sand. The intra-particle diffusion rate coefficient had a very small value of $(4.52 \pm 0.38) \times 10^{-7}$ mol g^{-1} $min^{-0.5}$.

Cr(VI) adsorption on clarified sludge, activated alumina, Fuller's earth and fly ash had pore diffusion rate coefficient in the range of 0.129 to 0.2198 mg g^{-1} $min^{-0.5}$, but the plots did not fully conform to the Eq. (13) as none of the plots pass through the origin [161]. It was likely that both surface adsorption and pore adsorption through intra-particle diffusion occurred simultaneously. Adsorption of Cr(III) and Cr(VI) on hydrous titanium oxide [160] is a second order process, but intra-particle diffusion cannot be ignored completely. The intra-particle diffusion plots did not have linearity over the whole range of contact time, but linearity was maintained over short time intervals. Naiya et al. [151] have found that the application of intra-particle diffusion model to Cd(II) adsorption on clarified sludge resulted in arriving at a very high pore diffusion rate coefficient of 6.40×10^2 mg g^{-1} min^{-05} (r~0.93), but the overall process could not be summarized as pore diffusion controlled. Similar results were obtained by Ghazy and Gad [137] for adsorption of Zn(II) on marble waste powder with a diffusion rate coefficient of 42.09 mg g^{-1} min^{-1}.

It is found that while the main mechanism of adsorption of metal ions on various inorganic solids may be mostly second order and occasionally first order, the initial uptake always has a strong presence of intra-particle diffusion. Most authors thus find that diffusion into pores plays a significant role in the rate processes and hence, computed the diffusion rate coefficient. Thus, Pb(II) adsorbed on modified bentonite (treated by 8-hydroxy quinoline) [60] with a diffusion rate coefficient of 1.024 to 1.280 mg g^{-1} $min^{-0.5}$ up to 60 min for the temperature range of 293 to 323 K with initial Pb(II) of 112.5 mg L^{-1}; both Pb(II) and Cd(II) adsorbed on activated alumina [156] with diffusion rate coefficient of 0.1060 to 0.5094 mg g^{-1} $min^{-0.5}$ for Cd(II)-alumina and from 0.1489 to 0.6440 mg g^{-1} $min^{-0.5}$ for Pb(II)-alumina for Pb(II) and Cd(II) concentrations of 10 to 50 mg L^{-1}; Cd(II) on loess soil [134] had intra-particle diffusion rate coefficient of 0.048 (Cd(II) 50 mg L^{-1}) and 0.054 mg g^{-1} $min^{-0.5}$ (Cd(II) 100 mg L^{-1}); Pb(II) on montmorillonite–illite type clay [186] had diffusion rate coefficient of 1.9855 to 3.1259 mg g^{-1} $min^{-0.5}$ for Pb(II) concentration of 100 to 200 mg L^{-1}; adsorption of Cu(II) on 2,2′-dipyridyl treated bentonite [173] had intra-particle diffusion rate coefficient of 0.448 to 0.140 mg g^{-1} min^{-1} in the temperature range of 293 to 323 K. The intra-particle diffusion model was also applied to Zn(II) adsorption on kaolin [197] without any quantitative findings. In all the cases, the plots had good linearity but they did not pass through the origin clearly overruling intra-particle diffusion as the sole rate determining process.

In a very recent study, Rodrigues et al. [164] applied the intra-particle diffusion model to Cr(VI) adsorption on $ZrO_2.nH_2O$ and observed that the plots are not linear over the whole time range, implying that more than one process affects Cr(VI) removal.

Adsorption of Cd(II), Co(II), Cu(II), Fe(III), Pb(II) and Ni(II)) on kaolinite, montmorillonite, and their modified forms (treated with tetrabutylammonium bromide, zirconium oxychloride, and 0.25 M

sulphuric acid) and of anionic Cr(VI) on kaolinite and its modified forms (treated with tetrabutylammonium bromide, zirconium oxychloride, and 0.25 M sulphuric acid) [147,158,165,171,175,188,201,205,206] has been principally proposed as following second order kinetics, but in all cases, intra-particle diffusion did play some significant role. Typical results are shown in Figs. 10 and 11. The non-zero intercepts of the plots in each case are a clear indication that although intra-particle diffusion is slow, it is not the slowest of the rate processes that determines the overall order. The interaction of metal ions with the clay surface remains the most significant rate process.

3.5. Film diffusion

Liquid film diffusion as a model for adsorption kinetics has not received much attention. A few reports in the literature appearing during the last few years are discussed below (Table 5, Appendix).

Gupta et al. [207] observed that the adsorption of As(III) on iron oxide coated sand followed liquid film diffusion mechanism. In adsorption of Cd(II) on clarified sludge, Naiya et al. [151] have investigated the influence of the liquid film diffusion model and the value of the diffusion coefficient was found to be 2.3×10^{-11} m^2 s^{-1}. However, these authors used a different version of the Eq. (14) and plotted $\ln[1/(1-F^2(t))]$ versus t to obtain the diffusion coefficient D from the slope, $\pi^2 D_e/r^2$. These authors have found that the pseudo second order model is generally valid for the experimental data, but the very low diffusion coefficient indicates that the cations are transferred through the liquid film surrounding the particles in a slow process and therefore, should influence the adsorption process. Similarly, adsorption of Cd(II) and Pb(II) on activated alumina [156] was found to possess a diffusion coefficient of 1.906×10^{-10} and 1.39×10^{-10} m^2 s^{-1}, respectively.

The film diffusion was the mechanism controlling the rate of Co(II) uptake onto NiO [208]. The values of diffusion coefficient were found to be 4.00×10^{-3}, 5.60×10^{-3} and 8.60×10^{-3} min^{-1} at 303, 313 and 323 K, respectively. The diffusion rate coefficient increased with rise in temperature since the ions become more energetic and reach the solid surface easily. The liquid film diffusion model was also used to explain the kinetics of adsorption of Pb(II) on montmorillonite–illite clay [186]. The validity of the model according to Eq. (14) is based on obtaining a zero intercept for the plots of $-\ln(1-F)$ vs. t, and it is

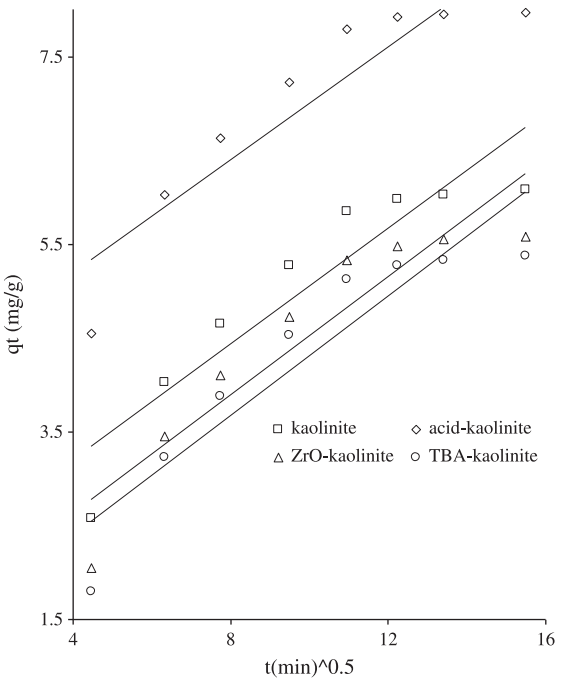

Fig. 11. Intraparticle diffusion plots for Cr(VI) on natural and modified kaolinite (experimental conditions: adsorbent 2 g L^{-1}, Cr(VI) 50 mg L^{-1}, temperature 303 K, and pH 4.6).

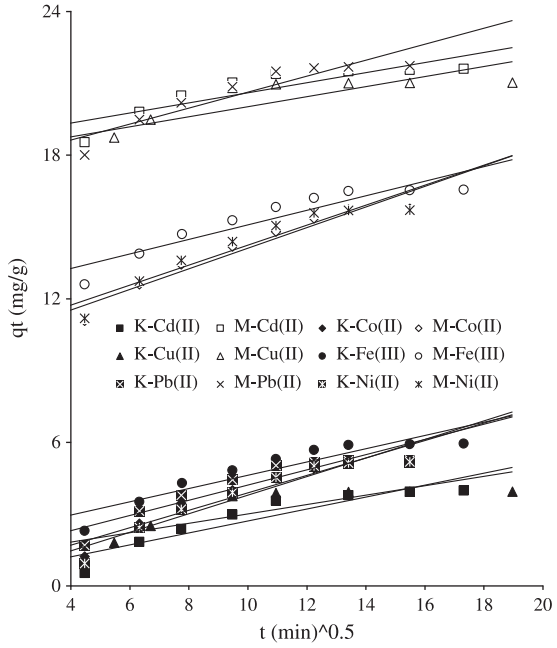

Fig. 10. Intraparticle diffusion plots for Cd(II), Co(II), Cu(II), Fe(III), Pb(II) and Ni(II) on kaolinite (K) and montmorillonite (M) (experimental conditions: adsorbent 2 g L^{-1}, metal ion 50 mg L^{-1}, temperature 303 K, and pH 5.5 for Cd(II), 5.8 for Co(II), 5.7 for Cu (II), 3.0 for Fe(III), 5.7 for Pb(II) and 5.7 for Ni(II)).

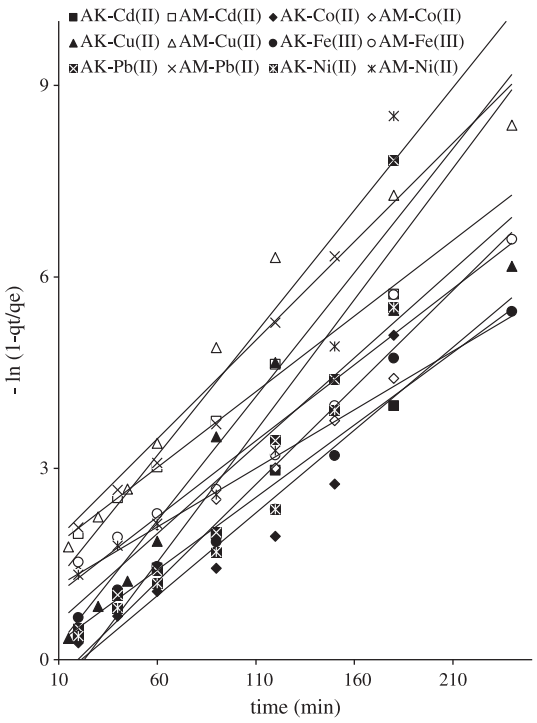

Fig. 12. Liquid film diffusion plots for Cd(II), Co(II), Cu(II), Fe(III), Pb(II) and Ni(II) on kaolinite (K) and montmorillonite (M) (experimental conditions: adsorbent 2 g L^{-1}, metal ion 50 mg L^{-1}, temperature 303 K, and pH 5.5 for Cd(II), 5.8 for Co(II), 5.7 for Cu (II), 3.0 for Fe(III), 5.7 for Pb(II) and 5.7 for Ni(II)).

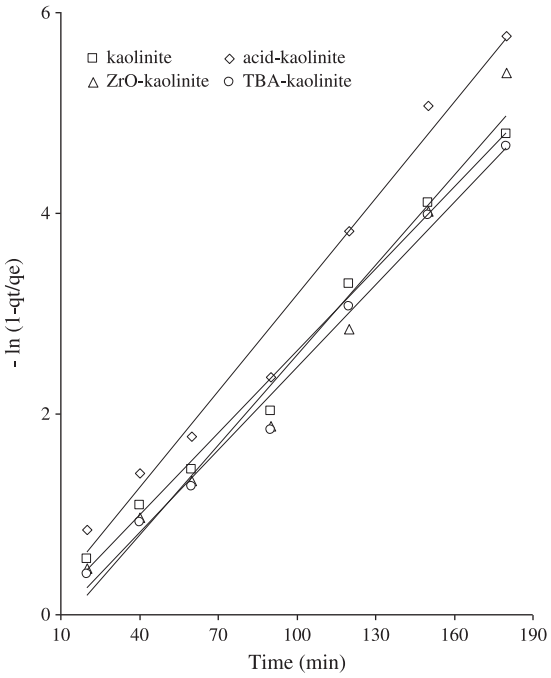

Fig. 13. Liquid film diffusion plots for Cr(VI) on natural and modified kaolinite (experimental conditions: adsorbent 2 g L^{-1}, Cr(VI) 50 mg L^{-1}, temperature 303 K, and pH 4.6).

found that when Pb(II) concentration was 200 mg L^{-1}, the intercept is almost zero (0.0085) intercept and therefore, at least in this particular case, the adsorption process was likely to be film-diffusion controlled. The film diffusion rate coefficient had a value of 0.0509.

Liquid film diffusion model was applied in each case to the kinetics of adsorption of Cd(II), Co(II), Cu(II), Fe(III), Pb(II), Ni(II) on kaolinite, montmorillonite and their modified forms (each treated with tetrabutylammonium bromide, zirconium oxychloride, and 0.25 M sulphuric acid) and of anionic Cr(VI) on kaolinite and its modified forms (treated similarly) [158,165,175,188,205,206]. The plots were linear (Figs. 12 and 13) and the lines were very close to passing through origin. Thus, liquid film diffusion could not be ruled out in the adsorption processes and the kinetics is likely to be diffusion-limited.

4. Conclusions

From the large number of recent works reviewed here, it is observed that the mechanism and kinetics of adsorption of metal cations and anions on inorganic adsorbents depend on the chemical nature of the materials and the experimental conditions, viz., ion concentration, adsorbent amount, pH and temperature of the medium. The pseudo first order model has been almost universally tested, but the validity has remained doubtful in many cases because of large discrepancy between the experimental and the computed values of equilibrium adsorption capacity. Part of the difficulties might be due to the uncertainty in the determination of the equilibrium adsorption capacity. Although not universally tested, it is found that in most cases of adsorption of metal cations on inorganic solids, the second order kinetics yields better results. Additional kinetic models like the Elovich equation, intra-particle diffusion model, and liquid film diffusion model have been tested only sparingly with various degrees of success.

On the basis of the results obtained by various groups of workers, it is not possible to classify the adsorbents into groups that conform to a particular kinetic model for the adsorption of the ions. The following observations, not generalizations, can be made from the large number of published works:

(i) Inorganic adsorbents like natural and modified $AlPO_4$ for Cd (II); beach sand for Cu(II) and Pb(II); ion exchange resin for Co (II), Cr(III), and Ni(II); red mud for As(III), As(V), Pb(II), and Cr (VI); rectorite for Cr(VI) etc., follow Lagergren first order kinetics.

(ii) A good number of adsorbents, viz, activated alumina for As(V), Cd(II), Cr(VI), and Pb(II); Al_2O_3 for Cd(II); MCM-41 for Ni(II); sludge for Cd(II) and Cr(VI); clinoptilolite for Ni(II); perlite for Cd(II); natural and modified magnetite nano-particles for As (V) and Cr(VI); hydrated ZrO_2 for Cr(VI); hydrated ferric oxide for As(V), etc., give better results with the second order kinetics.

(iii) A variety of natural and modified clays (kaolinite, montmorillonite, and bentonite) adsorb different metal cations (e.g. Cd (II), Cu(II), Co(II), Cr(III), Cr(VI), Co(II), Fe(III), Pb(II), Ni(II), etc.) following the second order kinetics. However, the removal of Cu(II), Co(II), Mn(II), and Ni(II) by kaolinite and Cu(II), Cr (III), and Zn(II) by sodium-dodecylsulfate-montmorillonite has followed the Lagergren first order kinetics.

(iv) The waste material, fly ash takes up metals like Cr(VI), Hg(II), Ni(II), and Zn(II) in accordance with the Lagergren first order mechanism while some authors have shown that the interactions with Cr(VI) can also follow second order kinetics. Such dual mechanisms have also been observed with TiO_2 adsorbent, which takes up Ni(II) through a first order mechanism while the removal of Cr(III), Cr(VI), and Se(VI) by TiO_2 has been shown to follow second order kinetics.

(v) In cases where the second order kinetics is applicable, the Elovich equation has also been shown to be an appropriate model. The interactions of Cd(II), Co(II), Cr(VI), Fe(III), Ni(II), and Pb(II) with natural and modified clays and Cr(III), Cr(VI), and Ni(II) with TiO_2 could be explained on the basis of the Elovich equation.

(vi) While diffusion processes are likely to considerably influence the adsorption kinetics in case of porous sorbents, this aspect has not received the desired attention. Some of the works have shown that both pore diffusion and liquid film diffusion play a role in the adsorbate–adsorbent interactions without going into details. Thus, the two processes are found to be important in uptake of Cd(II), Co(II), Cr(VI), Fe(III), Ni(II), and Pb(II) on natural/modified kaolinite and montmorillonite, while in some cases, either the intra-particle diffusion process, e.g., Cr(VI) and Cu(II) on activated alumina; Cr(VI), Ni(II), and Zn(II) on natural/modified fly ash; Cr(III) and Cr(VI) on TiO_2; or the liquid film diffusion model e.g., Co(II) on NiO, has only been tested.

Supplementary materials related to this article can be found online at doi:10.1016/j.cis.2010.12.004.

Acknowledgements

The authors are grateful to the University Grants Commission, India for sponsoring a substantial part of this work. The authors are also thankful to the reviewers for very useful comments and suggestions.

References

[1] Thomas WJ, Crittenden B. Adsorption technology and design. Oxford: Butterworth-Heinemann; 1998. p. 8–30.
[2] Gupta VK, Mohan D, Sharma S. Sep Sci Technol 1998;33:1331.
[3] Gupta VK, Jain CK, Ali I, Sharma M, Saini VK. Water Res 2003;37:4038.
[4] Mercer KL, Tobiason JE. Environ Sci Technol 2008;42:3797.
[5] Lafferty BJ, Loeppert RH. Environ Sci Technol 2005;39:2120.

[6] Ozmen M, Can K, Arslan G, Tor A, Cengeloglu Y, Ersoz M. Desalination 2010;254:162.
[7] Liu YT, Wang MK, Chen TY, Chiang PN, Huang PM, Lee JF. Environ Sci Technol 2006;40:7784.
[8] Northcott K, Kokusen H, Komatsu Y, Stevens G. Sep Sci Technol 2006;41:1829.
[9] Gupta VK, Sharma S. Ind Eng Chem Res 2003;42:6619.
[10] Ho YS, McKay G, Wase DAJ, Forster CF. Ads Sci Technol 2000;18:639.
[11] Ho YS, Ng JCY, McKay G. Sep Sci Technol 2001;36:241.
[12] Özer A, Özer D, Ekiz Hİ. Adsorption 2004;10:317.
[13] Loukidou MX, Karapantsios TD, Zouboulis AI, Matis KA. Sep Sci Technol 2005;40:1293.
[14] Gupta VK, Rastogi A, Saini VK, Jain N. J Colloid Interface Sci 2006;296:59.
[15] Gupta VK, Rastogi A. J Hazard Mater 2008;152:407.
[16] Pérez-Marín AB, Meseguer Zapata V, Ortuño JF, Aguilar M, Sáez J, Lloréns M. J Hazard Mater 2007;139:122.
[17] Gupta VK, Rastogi A. J Hazard Mater 2008;154:347.
[18] Wang XS, Tang YP, Tao SR. Adsorption 2008;14:823.
[19] Fiol N, Escudero C, Villaescusa I. Sep Sci Technol 2008;43:582.
[20] Gupta VK, Rastogi A. J Hazard Mater 2008;153:759.
[21] Gupta VK, Rastogi A. J Hazard Mater 2009;163:396.
[22] Gupta VK, Rastogi A, Nayak A. J Colloid Interface Sci 2010;342:533.
[23] Wang X-S, Qin Y, Li Z-F. Ind Eng Chem Res 2009;48:3589.
[24] Vijayaraghavan K, Arun M, Joshi UM, Balasubramanian R. Ind Eng Chem Res 2009;48:3589.
[25] Gerente C, Lee VKC, Le Cloirec P, McKay G. Crit Rev Environ Sci Technol 2007;37:41.
[26] Ho Y-S. J Hazard Mater 2006;B136:681.
[27] Bhattacharyya KG, Sen Gupta S. Adv Colloid Interface Sci 2008;140:114.
[28] Febrianto J, Kosasih AN, Sunarso J, Ju Y-H, Indraswati N, Ismadji S. J Hazard Mater 2009;162:616.
[29] Gupta VK, Carrott PJM, Ribeiro Carrott MML, Suhas. Crit Rev Environ Sci Technol 2009;39:783.
[30] Lagergren S. Kungliga Svenska Vetenskapsakademiens, Handlingar, Band 1898;24(4):1.
[31] Ungarish M, Aharoni C. J Chem Soc Faraday Trans 1981;77:975.
[32] McKay G, Ho YS, Ng JCY. Sep Purif Methods 1999;28:87.
[33] Allen SJ, Gan Q, Matthews R, Johnson PA. J Colloid Interface Sci 2005;286:101.
[34] Febrianto J, Kosasih AN, Sunarso J, Ju Y-H, Indraswati N, Ismadji S. J Hazard Mater 2009;162:616.
[35] Plazinski W, Rudzinski W, Plazinska A. Adv Colloid Interface Sci 2009;152:2.
[36] Ho YS, McKay G. Trans I Chem E 1998;76B:332.
[37] Ho YS, McKay G. Trans I Chem E 1999;77B:165.
[38] Ho YS, McKay G. Water Res 2000;34:735.
[39] Rudzinski W, Plazinski W. Adsorption 2009;15:181.
[40] Azizian S. J Colloid Interface Sci 2004;276:47.
[41] Rudzinski W, Plazinski W. J Phys Chem 2006;B110:16514.
[42] Ho YS, McKay G. Ads Sci Technol 1998;16:243.
[43] Al-Ghouti MA, Khraisheh MAM, Ahmad MNM, Allen S. J Hazard Mater 2009;165:589.
[44] Nandi BK, Goswami A, Purkait MK. J Hazard Mater 2009;161:387.
[45] Kennedy LJ, Vijaya JJ, Sekaran G, Kayalvizhi K. J Hazard Mater 2007;149:134.
[46] Alkan M, Demirbaş Ö, Doğan M. Micro Meso Mater 2007;101:388.
[47] Hamdaoui O, Saoudi F, Chiha M, Naffrechoux E. Chem Eng J 2008;143:73.
[48] Lin C-I, Wang L-H. J Chin Inst Chem Eng 2008;39:579.
[49] Rudzinsk W, Everett DH. Adsorption of gases on heterogeneous surfaces. London: Academic Press; 1992.
[50] Ho YS, McKay G. Ads Sci Technol 2002;20:797.
[51] Rudzinski W, Panczyk T. Adsorption 2002;8:23.
[52] Chien S, Clayton WR. Soil Sci Soc Am J 1980;44:265.
[53] Ruthven DM. Principal of adsorption and adsorption processes. New York: Wiley-Interscience; 1984.
[54] Banerjee K, Cheremisinoff PN, Cheng SL. Water Res 1997;31:249.
[55] Manju GN, Anoop Krishnan K, Vinod VP, Anirudhan TS. J Hazard Mater 2002;B9:221.
[56] Weber WJ, Morris JC. J Sanit Eng Div Am Soc Civ Eng 1963;89:31.
[57] Boyd GE, Adamson AW, Myers Jr LS. J Am Chem Soc 1947;69:2836.
[58] Yin Y, Allen HE, Huang CP, Sparks DL, Sanders PF. Environ Sci Technol 1997;31:496.
[59] Wu F-C, Tseng R-L, Juang R-S. Water Res 2001;35:613.
[60] Özcan AS, Gök Ö, Özcan A. J Hazard Mater 2009;161:499.
[61] Weber Jr WJ, McGinley PM, Katz LE. Water Res 1991;25:499.
[62] Low KS, Lee CK, Liew SC. Process Biochem 2007;36:59.
[63] Ding P, Huang K-L, Li G-Y, Zeng W-W. J Hazard Mater 2007;146:58.
[64] Doula M, Ioannou A, Dimirkou A. Adsorption 2000;6:325.
[65] Al-Degs YS, Tutunju MF, Shawabkeh RA. Sep Sci Technol 2000;35:2299.
[66] Jobstmann H, Singh B. Water Air Soil Pollut 2001;131:203.
[67] Chantawong V, Harvey NW, Bashkin VN. Water Air Soil Pollut 2003;148:111.
[68] Pan S-C, Lin C-C, Tseng D-H. Resour Conserv Recycl 2003;39:79.
[69] Echeverría J, Indurain J, Churio E, Garrido J. Colloids Surf A Physicochem Eng Aspects 2003;218:175.
[70] Abollino O, Aceto M, Malandrino M, Sarzanini C, Mentasti E. Water Res 2003;37:619.
[71] Doušová B, Machovič V, Koloušek D, Kovanda F, Dorničák V. Water Air Soil Pollut 2003;149:251.
[72] Peld M, Tõnsuaadu K, Bender V. Environ Sci Technol 2004;38:5626.
[73] Erdem E, Karapinar N, Donat R. J Colloid Interface Sci 2004;280:309.
[74] Perić J, Trgo M, Medvidovic NV. Water Res 2004;38:1893.
[75] Zhang Y, Yang M, Dou X-M, He H, Wang D-S. Environ Sci Technol 2005;39:7246.
[76] Wingenfelder U, Nowack B, Furrer G, Schulin R. Water Res 2005;39:3287.
[77] Pena M, Meng X, Korfiatis GP, Jing C. Environ Sci Technol 2006;40:1257.
[78] Hajialigol S, Taher MA, Malekpour A. Ads Sci Technol 2006;24:487.
[79] Shawabkeh RA, Al-Khashman OA, Al-Omari HS, Shawabkeh AF. Environmentalist 2007;27:357.
[80] Iznaga IR, Petranovskii V, Fuentes GR, Mendoza C, Aguilar AB. J Colloid Interface Sci 2007;316:877.
[81] Kubilay Ş, Gürkan R, Savran A, Şahan T. Adsorption 2007;13:41.
[82] Sui Y, Wu D, Zhang D, Zheng X, Hu Z, Kong H. J Colloid Interface Sci 2008;322:13.
[83] Leyva-Ramos R, Jacobo-Azuara A, Diaz-Flores PE, Guerrero-Coronado RM, Mendoza-Barron J, Berber-Mendoza MS. Colloids Surf A Physicochem Eng Aspects 2008;330:35.
[84] Kocaoba S. Environ Eng Sci 2008;25:697.
[85] Guerra DL, Viana RR, Airoldi C. Mater Res Bull 2009;44:485.
[86] Kocaoba S. Desalination 2009;244:24.
[87] Šljivić M, Smičiklas I, Pejanović S, Plećaš I. Appl Clay Sci 2009;43:33.
[88] Zhao G, Zhang H, Fan Q, Ren X, Li J, Chen Y, et al. J Hazard Mater 2010;173:661.
[89] Arpa Ç, Say R, Şatiroğlu N, Bektaş S, Yürüm Y, Genç Ö. Turk J Chem 2000;24:209.
[90] Ćurković L, Cerjan-Stefanović Š, Rastovèan-Mioè A. Water Res 2001;35:3436.
[91] Bayat B. J Hazard Mater 2002;B95:275.
[92] Bayat B. J Hazard Mater 2002;B95:251.
[93] Chakir A, Bessiere J, Kacemi EL, Marouf B. J Hazard Mater 2002;95:29.
[94] Kara M, Yuzer H, Sabah E, Celik MS. Water Res 2003;37:224.
[95] Dey RK, Jha U, Patnaik T, Singh AC, Singh VK. Sep Sci Technol 2009;44:1829.
[96] Ghosh UC, Dasgupta M, Debnat S, Bhat SC. Water Air Soil Pollut 2003;143:245.
[97] Gupta VK, Singh P, Rahman N. J Colloid Interface Sci 2004;275:398.
[98] Kandah MI. Sep Purif Technol 2004;35:61.
[99] Northcott K, Kokusen H, Komatsu Y, Stevens G. Sep Sci Technol 2006;41:1829.
[100] Hammari LE, Laghzizil A, Saoiabi A, Barboux P, Meyer M, Brandès S, et al. Ads Sci Technol 2006;24:507.
[101] Sari A, Tuzen M, Soylak M. J Hazard Mater 2007;144:41.
[102] Karabelli D, Üzüm Ç, Shahwan T, Eroğlu AE, Scott TB, Hallam KR, et al. Ind Eng Chem Res 2008;47:4758.
[103] Abu-Eishah SI. Appl Clay Sci 2008;42:201.
[104] Maxim K, Valeri K, Yuri K. J Environ Sci 2008;20:827.
[105] Nasef MM, Yahaya AH. Desalination 2009;249:677.
[106] Dey RK, Jha U, Patnaik T, Singh AC, Singh VK. Sep Sci Technol 2009;44:1829.
[107] Frini-Srasra N, Srasra E. Desalination 2010;250:26.
[108] Xu Y-H, Nakajima T, Ohki A. J Hazard Mater 2002;B92:275.
[109] Genç-Fuhrman H, Tjell JC, Mcconchie D. Environ Sci Technol 2004;38:2428.
[110] Kanel SR, Manning B, Charlet L, Choi H. Environ Sci Technol 2005;39:1291.
[111] Singh AP, Srivastava KK, Shekhar H. Ind J Chem Technol 2009;16:136.
[112] Ghazy SE, Samra SE, Mahdy AM, El-Morsey SM. Sep Sci Technol 2005;40:1797.
[113] Gupta VK, Sharma S. Environ Sci Technol 2002;36:3612.
[114] Abou-Mesalam MM. Colloids Surf A Physicochem Eng Aspects 2003;225:85.
[115] Abou-Mesalam MM. Adsorption 2004;10:87.
[116] Yun L, Pingxiao W, Zhi D, Daiqi Y. Acta Geol Sin 2006;80:219.
[117] Mustafa S, Javid M, Zaman MI. Sep Sci Technol 2009;44:304.
[118] Gupta VK, Gupta M, Sharma S. Water Res 2001;35:1125.
[119] Rengaraj S, Yeon K-H, Kang S-Y, Lee J-U, Kim K-W, Moon S-H. J Hazard Mater 2002;B92:185.
[120] Banerjee SS, Joshi MV, Jayaram RV. Sep Sci Technol 2004;39:1611.
[121] Huang Y, Ma X, Liang G, Yan Y, Wang S. Chem Eng J 2008;138:187.
[122] Weng C-H, Sharma YC, Chu S-H. J Hazard Mater 2008;155:65.
[123] Carnizello AP, Marçal L, Calefi PS, Nassar EJ, Ciuffi KJ, Trujillano R, et al. J Chem Eng Data 2009;54:241.
[124] Yavuz Ö, Altunkaynak Y, Güzel F. Water Res 2003;37:948.
[125] Lin S-H, Juang R-S. J Hazard Mater 2002;B92:315.
[126] Ghazy SE, Ragab AH. Ind J Chem Technol 2007;14:507.
[127] Karamanis D, Assimakopoulos PA. Water Res 2007;41:1897.
[128] Tofan L, Paduraru C, Bilba D, Rotariu M. J Hazard Mater 2008;156:1.
[129] Prasad M, Saxena S, Amritphale SS, Chandra N. Ind Eng Chem Res 2000;39:3034.
[130] Taqvi SIH, Bhanger MI, Shah SW. Sep Sci Technol 2006;41:531.
[131] Ahmed R, Yamin T, Ansari MS, Hasany SM. Ads Sci Technol 2006;24:475.
[132] Liu Y, Xiao D, Li H. Sep Sci Technol 2007;42:185.
[133] Xu HY, Yang L, Wang P, Liu Y, Peng MS. J Environ Manage 2008;86:319.
[134] Banerjee SS, Jayaram RV, Joshi MV. Sep Sci Technol 2003;38:1015.
[135] Debnath S, Ghosh UC. Chem Eng J 2009;152:480.
[136] Heidari A, Younesi H, Mehraban Z. Chem Eng J 2009;153:70.
[137] Ghazy SE, Gad AHM. Ind J Chem Technol 2008;15:433.
[138] Taqvi SIH, Hasany SM, Bhanger MI. Sep Purif Technol 2008;61:153.
[139] Maity S, Chakravarty S, Bhattacharjee S, Roy BC. Water Res 2005;39.
[140] Giménez J, Martínez M, de Pablo J, Rovira M, Duro L. J Hazard Mater 2007;141:575.
[141] Maiti A, DasGupta S, Basu JK, De S. Ind Eng Chem Res 2008;47:1620.
[142] Yu M-J, Li X, Ahn W-S. Micro Meso Mater 2008;113:197.
[143] Zhang Q, Pan B, Zhang W, Pan B, Zhang Q, Ren H. Ind Eng Chem Res 2008;47:3957.
[144] Mathialagan T, Viraraghavan T. J Hazard Mater 2002;94:291.
[145] Dal Bosco SM, Jimenez RS, Vignado C, Fontana J, Geraldo B, Figueiredo FCA, et al. Adsorption 2006;12:133.
[146] Sen Gupta S, Bhattacharyya KG. J Hazard Mater 2006;B128:247.
[147] Bhattacharyya KG, Sen Gupta S. Ind Eng Chem Res 2007;46:3734.
[148] Yu R, Wanga S, Wang D, Ke J, Xing X, Kumada N, et al. Catal Today 2008;139:135.
[149] Unuabonah EI, Adebowale KO, Olu-Owolabi BI, Yang LZ. Adsorption 2008;14:791.

[150] Sen TK, Sarzali MV. Chem Eng J 2008;142:256.
[151] Naiya TK, Bhattacharya AK, Das SK. J Colloid Interface Sci 2008;325:48.
[152] Wu P, Wu W, Li S, Xing N, Zhu N, Li P, et al. J Hazard Mater 2009;169:824.
[153] Unuabonah EI, Adebowale KO, Ofomaja AE. Water Air Soil Pollut 2009;200:133.
[154] Panuccio MR, Sorgonà A, Rizzo M, Cacco G. J Environ Manage 2009;90:364.
[155] Wang Y, Tang X, Chen Y, Zhan L, Li Z, Tang Q. J Hazard Mater 2009;172:30.
[156] Naiya TK, Bhattacharya AK, Das SK. J Colloid Interface Sci 2009;333:14.
[157] Liang X, Xu Y, Sun G, Wang L, Sun Y, Qin X. Colloids Surf A Physicochem Eng Aspects 2009;349:61.
[158] Bhattacharyya KG, Sen Gupta S. Ind Eng Chem Res 2006;45:7232.
[159] Sari A, Tuzen M. Sep Sci Technol 2008;43:3563.
[160] Debnath S, Ghosh UC. J Chem Thermodyn 2008;40:67.
[161] Bhattacharya AK, Naiya TK, Mandal SN, Das SK. Chem Eng J 2008;137:529.
[162] Yuan P, Fan M, Yang D, He H, Liu D, Yuan A, et al. J Hazard Mater 2009;166:821.
[163] Yuan P, Liu D, Fan M, Yang D, Zhu R, Ge F, et al. J Hazard Mater 2010;173:614.
[164] Rodrigues LA, Maschio LJ, da Silva RE, da Silva MLCP. J Hazard Mater 2010;173:630.
[165] Bhattacharyya KG, Sen Gupta S. Sep Sci Technol 2007;42:3391.
[166] Bhattacharyya KG, Sen Gupta S. Colloids Surf A Physicochem Eng Aspects 2008;317:71.
[167] Bhattacharyya KG, Sen Gupta S. Appl Clay Sci 2009;46:216.
[168] Anirudhan TS, Suchithra PS. Chem Eng J 2010;156:146.
[169] Wang X-S, Wang J, Sun C. Ads Sci Technol 2006;24:517.
[170] Bhattacharyya KG, Sen Gupta S. Sep Purif Technol 2006;50:388.
[171] Bhattacharyya KG, Sen Gupta S. Chem Eng J 2008;136:1.
[172] Weng C-H, Tsai C-Z, Chu S-H, Sharma YC. Sep Purif Technol 2007;54:187.
[173] Erdem B, Özcan A, Gök Ö, Özcan AS. J Hazard Mater 2009;163:418.
[174] Manu V, Mody HM, Bajaj HC, Jasra RV. Ind Eng Chem Res 2009;48:8954.
[175] Bhattacharyya KG, Sen Gupta S. Adsorption 2006;12:185.
[176] Bektaş N, Kara S. Sep Purif Technol 2004;39:189.
[177] Sen Gupta S, Bhattacharyya KG. Appl Clay Sci 2005;30:199.
[178] Bhattacharyya KG, Sen Gupta S. Colloids Surf A Physicochem Eng Aspects 2006;277:191.
[179] Sari A, Tuzen M, Citak D, Soylak M. J Hazard Mater 2007;149:283.
[180] Huang Y-H, Hsueh C-L, Huang C-P, Su L-C, Chen C-Y. Sep Purif Technol 2007;55:23.
[181] Zhang SQ, Hou WG. Colloids Surf A Physicochem Eng Aspects 2008;320:92.
[182] Şölener M, Tunali S, Özcan AS, Özcan A, Gedikbey T. Desalination 2008;223:308.
[183] Wang XS, He L, Hu HQ, Wang J. Sep Sci Technol 2008;43:908.
[184] Wang S, Dong Y, He M, Chen L, Yu X. Appl Clay Sci 2009;43:164.
[185] Fan Q, Li Z, Zhao H, Jia Z, Xu J, Wu W. Appl Clay Sci 2009;45:111.
[186] Oubagaranadin JUK, Murthy ZVP. Ind Eng Chem Res 2009;48:10627.
[187] Liu S-Y, Gao J, Yang Y-J, Yang Y-C, Ye Z-X. J Hazard Mater 2010;173:558.
[188] Sen Gupta S, Bhattacharyya KG. J Colloid Interface Sci 2006;295:21.
[189] Bhattacharyya KG, Sen Gupta S. Sep Sci Technol 2008;43:3221.
[190] Rengaraj S, Yeon J-W, Kim Y, Kim W-H. Ind Eng Chem Res 2007;46:2834.
[191] Argun ME. J Hazard Mater 2008;150:587.
[192] Carvalho WA, Vignado C, Fontana J. J Hazard Mater 2008;153:1240.
[193] Mandal S, Mayadevi S, Kulkarni BD. Ind Eng Chem Res 2009;48:7893.
[194] Shi K, Wang X, Guo Z, Wang S, Wu W. Colloids Surf A Physicochem Eng Aspects 2009;349:90.
[195] Balkaya N, Cesur H. J Sci Ind Res 2008;67:254.
[196] Guerra DL, Airoldi C, Lemos VP, Angélica RS. J Hazard Mater 2008;155:230.
[197] Arias F, Sen TK. Colloids Surf A Physicochem Eng Aspects 2009;348:100.
[198] Tang X, Li Z, Chen Y, Wang Z. Desalination 2009;249:49.
[199] Nibou D, Mekatel H, Amokrane S, Barkat M, Trari M. J Hazard Mater 2010;173:637.
[200] Cortés-Martínez R, Martínez-Miranda V, Solache-Ríos M, García-Sosa I. Sep Sci Technol 2004;39:2711.
[201] Sen Gupta S, Bhattacharyya KG. J Environ Manage 2008;87:46.
[202] Gupta VK, Ali I. Sep Purif Technol 2000;18:131.
[203] Gupta VK, Ali I. J Colloid Interface Sci 2004;271:321.
[204] Rengaraj S, Kim Y, Joo CK, Yi J. J Colloid Interface Sci 2004;273:4.
[205] Bhattacharyya KG, Sen Gupta S. Ads Sci Technol 2009;27:47.
[206] Bhattacharyya KG, Sen Gupta S. J Colloid Interface Sci 2007;310:411.
[207] Gupta VK, Saini VK, Jain N. J Colloid Interface Sci 2005;288:55.
[208] Naeem A, Saddique MT, Mustafa S, Tasleem S, Shah KH, Waseem M. J Hazard Mater 2009;172:124.